



ALMA MATER STUDIORUM
UNIVERSITÀ DI BOLOGNA

ARCHIVIO ISTITUZIONALE DELLA RICERCA

Alma Mater Studiorum Università di Bologna Archivio istituzionale della ricerca

Economic and environmental benefits by improved process control strategies in HCl removal from waste-to-energy flue gas

This is the final peer-reviewed author's accepted manuscript (postprint) of the following publication:

Published Version:

Dal Pozzo A., Muratori G., Antonioni G., Cozzani V. (2021). Economic and environmental benefits by improved process control strategies in HCl removal from waste-to-energy flue gas. WASTE MANAGEMENT, 125, 303-315 [10.1016/j.wasman.2021.02.059].

Availability:

This version is available at: <https://hdl.handle.net/11585/821276> since: 2021-05-31

Published:

DOI: <http://doi.org/10.1016/j.wasman.2021.02.059>

Terms of use:

Some rights reserved. The terms and conditions for the reuse of this version of the manuscript are specified in the publishing policy. For all terms of use and more information see the publisher's website.

This item was downloaded from IRIS Università di Bologna (<https://cris.unibo.it/>).
When citing, please refer to the published version.

(Article begins on next page)

Economic and environmental benefits by improved process control strategies in HCl removal from waste-to-energy flue gas

HIGHLIGHTS

*Alessandro Dal Pozzo, Giacomo Muratori, Giacomo Antonioni, Valerio Cozzani**

LISES - Dipartimento di Ingegneria Civile, Chimica, Ambientale e dei Materiali, Alma Mater Studiorum - Università di Bologna, via Terracini n.28, 40131 Bologna, Italy

(*)*corresponding author*, Tel. +39-051-2090240, Fax +39-051-2090247, e-mail: valerio.cozzani@unibo.it

- A methodology was outlined to test control strategies in operating facilities
- A virtual console was used to reproduce system behaviour
- Environmental, Economic and Technical performance indicators were defined
- Improved control strategies result in higher Environmental and Economic performance
- Full-scale test-runs confirmed the effectiveness of alternative control strategies

1 Economic and environmental benefits by improved process control strategies in HCl removal
2 from waste-to-energy flue gas

3

4 *Alessandro Dal Pozzo, Giacomo Muratori, Giacomo Antonioni, Valerio Cozzani**

5 LISES - Dipartimento di Ingegneria Civile, Chimica, Ambientale e dei Materiali, Alma Mater
6 Studiorum - Università di Bologna, via Terracini n.28, 40131 Bologna, Italy

7

8 (*)*corresponding author*, Tel. +39-051-2090240, Fax +39-051-2090247, e-mail:
9 valerio.cozzani@unibo.it

10

11 Abstract

12 The control of HCl emission in waste-to-energy (WtE) facilities is a challenging flue gas
13 treatment problem: the release of HCl from waste combustion is highly variable in time and
14 the HCl emission standards are typically far lower in WtE than in any other industry.
15 Traditional process control approaches in dry HCl removal processes are generally based on
16 feeding a large excess of solid reactants to the system, to ensure robustness and a wide safety
17 margin in the compliance to environmental regulations. This results in the production of a
18 high amount of unreacted sorbents, strongly increasing the generation of solid wastes that
19 need to be disposed. In the present study, an approach was developed to allow the
20 implementation of improved control strategies for dry HCl abatement systems in operating
21 full-scale facilities. Its objective is the reduction of the reactant feed and the waste
22 production, while still providing an adequate safety margin for emission compliance. The
23 approach was based on the reproduction of the behaviour of the real system in a virtual
24 console that allows the extensive testing of alternative control strategies, limiting the need of
25 demanding test-runs at the real plant. A test case on an Italian WtE facility demonstrated the
26 capability of a control logic tuned in the virtual console to achieve a 13% reduction in the
27 consumption of reactants and generation of process residues, with unchanged HCl removal

28 efficiency. The results evidence the wide opportunities for optimisation of dry acid gas
29 removal systems, in particular when multistage systems are implemented.

30 **Keywords:** waste-to-energy, HCl, process optimization, dry sorbent injection.

31 1 Introduction

32 In a modern waste management system, waste-to-energy (WtE) facilities have the role to
33 divert from landfilling waste streams for which recycling is currently technically or
34 economically unfeasible (Nizami et al., 2016) and enabling their thermal valorisation (Arena
35 et al., 2015), thus facilitating the transition to a circular economy (Bagheri et al., 2020; Van
36 Caneghem et al., 2019). Thanks to increasingly ambitious environmental regulations, the
37 emission of several air pollutants related to WtE operation has been reduced more than
38 tenfold in the last decades (Ardolino et al., 2020; Damgaard et al., 2010). However, in the
39 current holistic approach to environmental protection, the reduction of impacts has to go
40 beyond the minimisation of the emission of pollutants at the stack of the plant. Also indirect
41 impacts, e.g. those associated to the consumption of reactants and the production of process
42 residues in the flue gas treatment system of the plant (Dal Pozzo et al., 2017; Dong et al.,
43 2020; Lausset et al., 2016), needs to be minimised.

44 Hydrogen chloride (HCl) is a typical pollutant in WtE flue gases, arising from the combustion
45 of waste containing chlorine (Zhang et al., 2019). Chlorine is widely dispersed amongst organic
46 and inorganic compounds present in several waste items (Gerassimidou et al., 2020; Yang et
47 al., 2018). Among the different techniques available for HCl removal (Bal et al., 2019; Dal
48 Pozzo et al., 2019; Ephraim et al., 2019; Kameda et al., 2020), dry sorbent injection (DSI) is
49 one of the technologies more frequently implemented (Beylot et al., 2018; Dal Pozzo et al.,
50 2018a). DSI consists in the in-duct addition of an alkaline powdered reactant (e.g. calcium

51 hydroxide or sodium bicarbonate), which neutralises acid pollutants as HCl via gas-solid
52 reaction (Antonioni et al., 2016). DSI, adopted in either single or two-stage configurations (Dal
53 Pozzo et al., 2016; De Greef et al., 2013), is considered among the best available techniques
54 for flue gas treatment in WtE installations recommended by the European Union (Neuwahl et
55 al., 2019).

56 The main environmental drawback of DSI systems is the high stoichiometric excess of reactant
57 feed that is required to achieve high HCl removal efficiency (Vehlow, 2015). The resulting
58 excess consumption of reactant leads to the generation of relevant streams of solid process
59 residues in the fabric filters, where they are collected together with fly ashes and
60 micropollutants. The presence of these other components in the collected process residues
61 causes the stream to be considered as hazardous waste and to require its disposal in
62 dedicated landfill sites (Dal Pozzo et al., 2018b; Kameda et al., 2020).

63 In addition, given that the composition of the waste burnt in the combustion chamber of a
64 WtE plant varies widely over time, the resulting extreme variability of HCl concentration at
65 the inlet of the flue gas treatment section (Dal Pozzo et al., 2020) is an inherent instability
66 that limits the effectiveness of conventional control strategies in calibrating the reactant feed
67 needed to maintain a constant concentration setpoint at the outlet. Thus, the prevailing trend
68 in control strategies is to calibrate the process control parameters of the DSI system on the
69 safe side, and even more so accept high excess feed rates of reactants to minimise the
70 possible occurrence of overruns of HCl emission limits at stack.

71 A more accurate setting of the DSI control system could ensure not only a safe compliance of
72 emission limits at stack, but also a reduction of the consumption of reactants and the
73 generation of process residues. These in principle represent an undesired environmental

74 burden shift between different compartments (from air to soil/water) (Bogush et al., 2015;
75 Margallo et al., 2015; Quina et al., 2018).

76 The problem of the optimisation of flue gas treatment control with reference either to the
77 WtE context or to acid pollutants (HCl, SO₂, HF) is scarcely addressed in scholarly literature.

78 Ting et al. (2008) described the design of a PID control for acid gas removal via semi-dry
79 scrubbing in a WtE plant, with parameter tuning performed during commissioning operation.

80 Gassner et al. (2014) explored the use of data-driven modelling approaches to describe the
81 non-stationary operational behaviour of a semi-dry flue gas desulfurization process. Cignitti

82 et al. (2016) developed a simple first principle model to predict the dynamics of a semidry SO₂
83 absorber in desulfurization units of coal-fired power plants, while Guo et al. (2019) used a

84 hybrid approach, blending first principles and neural network, to model and optimise a wet
85 flue gas desulfurization unit. Yet, the focus of these recent studies has been mainly the

86 theoretical development of enhanced dynamic models of the process, rather than their
87 implementation in real control schemes. In particular, to the best of the authors' knowledge,

88 no previous paper addresses the potential environmental and economic advantages in terms
89 of reduced reactant consumption and related waste generation achievable with process

90 control optimisation in WtE acid gas removal.

91 Furthermore, control optimisation in the WtE context is made complex by the fact that
92 conventional direct tuning via extensive test runs during plant operation is generally

93 incompatible with the need to comply with strict HCl emission limits in presence of a highly
94 variable inlet load of HCl coming from waste combustion. In this regard, the set-up of data-

95 driven simulations of the real system in a virtual environment, as more and more frequently
96 performed in the manufacturing (Goodall et al., 2019) and process industry (Kockmann,

97 2019), could drastically reduce the need of field tests. By this strategy, the screening and the

98 tuning of new control settings is carried out directly in a virtual set-up, thus limiting the
99 number of in-field test runs only to those needed for the initial calibration of the simulation
100 and for the final trial of the new control system.

101 The present study focuses on the development of an approach for the optimisation of process
102 control in a typical DSI system for HCl removal based on a virtual environment. A dynamic
103 simulation of the dry treatment system was built in a virtual console implemented using the
104 Simulink software. A data-driven process model, calibrated with a specific set of test data,
105 nested into a reproduction of the control system of the DSI unit, was thus obtained and
106 validated. The virtual console was used to test and tune an alternative control strategy, with
107 the objective to reduce the stoichiometric excess of reactant associated to HCl removal. The
108 alternative control was then tested in full scale at the real plant, demonstrating the potential
109 for significant environmental and economic benefits deriving from the reduction in reactant
110 consumption and related process waste generation.

111

112 2 Reference system and test facility

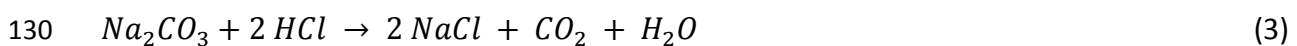
113

114 **2.1 HCl removal system**

115 The two-stage acid gas abatement system of a medium-sized (400 t/d of waste treated) WtE
116 facility located in Northern Italy was used as case study. As shown in Fig. 1, this system is
117 based on two consecutive steps of dry sorbent injection and filtration, taking place at ~180
118 °C, downstream of the heat recovery section of the plant. In the first stage, calcium hydroxide,
119 $\text{Ca}(\text{OH})_2$, is injected, triggering the following gas-solid reaction of HCl neutralisation (Iizuka et
120 al., 2020):



122 A fabric filter separates the solid product of reaction from the flue gas, together with a
123 relevant unreacted fraction of $\text{Ca}(\text{OH})_2$, present both due to the excess feed of reactant and
124 for the intrinsic diffusional limitations of gas-solid reaction (i.e. the phenomenon of
125 incomplete conversion discussed by Antonioni et al., 2016). In the second stage, the dry
126 injection is based on sodium bicarbonate, NaHCO_3 . At the injection temperature and, in
127 general, at $T > 130$ °C (see Hartman et al., 2013), NaHCO_3 decomposes to porous sodium
128 carbonate (Na_2CO_3), which in turn absorbs HCl (Dal Pozzo et al., 2019):



131 Again, the solid product of reaction and an unreacted fraction of reactant are collected by a
132 fabric filter. This two-stage configuration is adopted in several European WtE installations and
133 it is appreciated for its built-in redundancy in terms of emission control (De Greef et al., 2013)
134 and its flexibility that allows different repartitions of abatement demand between the two
135 stages (Dal Pozzo et al., 2016).

136 As shown in Fig. 1, the present study is focused on the optimisation of the control of the
137 Ca(OH)_2 1st stage of acid gas removal, referred to in the following as dry sorbent injection (DSI)
138 system. As discussed in the following, the optimisation and tuning of the process control of
139 the 1st stage not only improves the performance of the stage, but, stabilising the HCl outlet
140 concentration, it also favours the optimal performance of the 2nd stage.

141

142 **2.2 Process control**

143 In the test facility, a conventional process control scheme implemented in several similar
144 plants is present. The operation of the two-stage acid gas abatement system is monitored by
145 the continuous acquisition of flue gas composition data at the measurement points PM1, PM2
146 and EM indicated in Fig. 1. The concentration of the main gas species at the sampling points,
147 including the acid pollutants (HCl, SO_2 , HF), is measured by Fourier-Transform infrared (FTIR)
148 spectrometry, in compliance with CEN/TS 17337 (CEN, 2019), while the flue gas flowrate is
149 determined at stack (point EM) by means of S-type Pitot tube velocity measurements.

150 In both the acid gas abatement stages, the distributed control system (DCS) of the plant
151 controls the solid reactant feed based on the measured inlet and outlet mass flowrates of
152 acid pollutants. A conditional logic selects the reactant feed rate as the maximum of two
153 values, calculated as follows:

- 154 i. *Feedforward criterion.* The calculated feed rate is equal to the stoichiometric demand
155 related to the abatement of the inlet mass flowrates of acid pollutants at PM1,
156 increased by a 10% excess.
- 157 ii. *Feedback criterion.* The feed rate is calculated according to a Proportional Integral (PI)
158 feedback formula based on the difference between a set-point for the outlet HCl
159 concentration and the value measured at PM2.

160 The settings of the feedback control (proportional gain $K_p = 5$ and integral gain $\tau_I = 8$ s)
161 provide an aggressive reaction, i.e. strong excess feed rates of reactant are delivered
162 whenever the outlet HCl concentration exceeds the setpoint. Conversely, when the outlet HCl
163 concentration is lower than the setpoint, the feed rate of reactant does not drop as
164 significantly, because the feedforward criterion takes over. Thus, the combination of the
165 feedforward and feedback criteria as detailed above realises an asymmetrical control action,
166 in which the setpoint is actually treated as a threshold. The feedforward PI control works
167 merely as an environmental safeguard, intended to act only if the feedforward is not capable
168 to maintain the outlet below the given threshold. A survey carried out by the authors involving
169 several Italian companies (HERAmbiente, HestAmbiente, IREN, Brianza Energia Ambiente)
170 evidenced that this control strategy is typical of WtE acid gas abatement units, as the
171 objective is to avoid any spike in outlet HCl resulting from a variation in the inlet HCl load
172 coming from waste combustion (Muratori et al., 2020).

173

174 **2.3 Drawbacks of the reference control system**

175 The typical behaviour of the control system described in section 2.2 is shown in Fig. 2. Most
176 of the time the control operates in feedforward mode and the feed rate of solid reactant is
177 proportional to the inlet HCl load. However, when the outlet HCl flowrate exceeds its setpoint,
178 the feedback mode takes over, imposing a relevant excess in feed rate to bring the HCl outlet
179 back under the threshold as soon as possible. This behaviour determines a peak in reactant
180 consumption but generates also unintended instability in the outlet HCl flow rate. As
181 pinpointed by the arrows in Fig. 2, the spike of reactant feed manages to quickly reduce the
182 outlet HCl flow rate, but such a reduction is often followed by a swift rebound of outlet HCl
183 to high values that triggers another activation of the feedback control, resulting in another

184 spike of reactant feed. Since the layers of solid reactant accumulated over time on the fabric
185 filter are known to play a major role in the overall acid gas removal action (Kim et al., 2017;
186 Wu et al., 2004), the spikes of reactant feed might be detrimental because they induce
187 unstable operation of the filter (Saleem and Krammer, 2012), activating frequent filter
188 cleaning and reducing the residence time of reactant on the filter. The unstable HCl flow rate
189 at the outlet of the 1st stage can in turn disturb the operation of the 2nd stage of acid gas
190 removal.

191 In general, this control does not include the minimisation of reactant feed as a criterion and
192 does not realise a rational use of reactant.

193

194 3 Methodology

195 3.1 Framework

196 Fig. 3 summarises the methodology developed to analyse the performance of alternative
197 process control strategies for DSI, aimed at environmental and economic optimisation. The
198 core element of the methodology is the development of a process simulation that allows
199 exploring alternative control settings in a virtual console, while reducing the need for full-
200 scale test-runs at the real plant. The process simulation duplicates into a software
201 environment the process units and the control system of the actual facility. As sketched in Fig.
202 3, building the simulation required: i) to reproduce the HCl removal process with a process
203 model; and ii) to simulate the control structure of the DSI unit. The first task required the
204 identification of an appropriate mathematical model for the description of the reaction
205 process (see section 3.2) and its training and validation on plant data collected from test-runs

206 (see section 3.3). The second task was performed replicating the control architecture of the
207 plant, briefly outlined in section 2.2, with a Simulink block diagram (see section 3.4).

208 The reliability of the simulation is validated considering the operating process control set-up
209 in the real plant and comparing the outputs of the simulation with those recorded in the plant
210 during normal operation, using the actual data as the input for the simulation. Once validated,
211 the simulation can be used to screen and tune alternative control strategies, eventually
212 leading to a new tuned control strategy that may be tested in the real plant, as in the test
213 case that will be introduced in section 4.

214 Besides conventional indicators of process control performance, specific environmental and
215 economic indicators (section 3.5) were defined to allow a comprehensive assessment of the
216 performance of the alternative control strategies.

217

218 **3.2 Selection of data-driven process model and input variables**

219 As mentioned above, a mathematical model is required to reproduce the process dynamics
220 in the simulation. The process model needs to predict how the instantaneous HCl removal
221 efficiency varies depending on the inlet HCl concentration and the feed of solid reactant.
222 Given the intrinsic unsteady nature of the process, this task can be addressed only with a
223 dynamic model capable of handling the rapidly changing operating conditions (e.g. variability
224 of HCl concentration due to variability of waste composition). Existing simplified stationary
225 models of acid gas removal that are typically applied for process optimisation studies
226 (Harriott, 1990; Dal Pozzo et al., 2016) are clearly not apt for this task. On the other hand,
227 phenomenological models (Antonioni et al., 2016; Foo et al., 2017; Montagnaro et al., 2016)
228 that describe rigorously the kinetic and mass transfer phenomena involved in the gas-solid
229 reaction process were typically derived from laboratory-scale data and are not suitable to

230 simulate full-scale systems, as stated by Gutiérrez Ortiz and Ollero (2008) and Gassner et al.
231 (2014).

232 Therefore, a data-driven approach was chosen. A system identification procedure was
233 performed to estimate the structure and the parameters of the model from observed input-
234 output plant data (Ljung, 2010). A simple input-output polynomial model, *i.e.* the linear auto-
235 regressive exogenous (ARX) model, was selected as base for the system identification. ARX
236 models have already demonstrated to be reliable tools in emission control problems, e.g. in
237 the prediction of NO_x (Smrekar et al., 2013) or SO_x (Choi et al., 2002) emissions from coal-
238 fired boilers. They are appreciated for their transparency and ease of interpretation (Akinola
239 et al., 2019). The general form of an ARX model is the following:

240

$$241 \quad y(t) = a_1 y(t-1) + \dots + a_{n_a} y(t-n_a) + \sum_i [b_{1,i} u_i(t-n_k) + \dots + b_{n_b,i} u_i(t-n_{k,i}-n_{b,i}+1)] + e(t) \quad (4)$$

242

243 where y is the output variable, u_i are the i input variables considered in the model, and e is
244 the white-noise disturbance value. The values a and b are the model parameters, which can
245 be represented in compact form in the parameter vector θ :

246

$$247 \quad \theta = [a_1 \dots a_{n_a} \ b_{1,i} \dots b_{n_b,i}]' \quad (5)$$

248

249 This model structure implies that the output variable y at time t is predicted as a linear
250 combination of past output values (autoregressive part of the model) and current and past
251 values of the input variables (exogenous part of the model). The parameters n_a and $n_{b,i}$ are,
252 respectively, the number of past output samples and the number of past input samples (for
253 each input variable i) considered for the prediction of the current output. The model can also

254 consider input delay terms $n_{k,i}$, i.e. the number of input samples that occur before the input
255 affects the output (also known as the dead time of the system). The use of past observations
256 in the prediction of the output allows approximating also derivative terms by difference
257 quotients, thus enabling the reproduction of the dynamics of the modelled system. The
258 numbers n_a , $n_{b,i}$ and $n_{k,i}$ are known as hyperparameters and represent the order of the model,
259 *i.e.* they indicate the number of parameters to optimise in the training of the model.

260 For the sake of simplicity, a two-input single-output ARX model was chosen for the present
261 study. The modelled output y is the HCl molar flowrate in the flue gas leaving the DSI system.
262 The two input variables u_i are the inlet HCl molar flowrate and the molar flowrate of $\text{Ca}(\text{OH})_2$
263 fed to the DSI system.

264 In general, other variables might also affect the HCl removal process. The second most
265 abundant acid compound in WtE flue gases, SO_2 , can consume a fraction of the reactant feed
266 (Zhang et al., 2019). Fluctuations in the flue gas flowrate can influence reactant residence
267 time (Hunt and Sewell, 2015). Variations in the operating temperature of the HCl removal
268 stage, e.g. caused by fouling in the heat recovery section upstream, can alter the gas-solid
269 reaction kinetics (Dal Pozzo et al., 2018c). However, variations of temperature and flue gas
270 flowrate are typically limited (see Fig. 2d and 2e) and, in the WtE plant under study, the inlet
271 SO_2 concentration was a couple of orders of magnitude lower than that of HCl. Therefore,
272 these variables were excluded in the formulation of the model.

273

274 **3.3 Calibration of the model**

275 As a data-driven model, the ARX structure requires a specific calibration on data from the
276 actual DSI system modelled. Informative data can be obtained by open-loop tests, in which

277 the control of the system is deactivated and process performance is assessed by varying
278 manually the feed rate of reactant while recording inlet and outlet HCl concentration.

279 The dataset Z^N , formed by N consecutive observations of the input and output variables,
280 obtained from the tests has to be divided in: i) a training set Z_{trn} , used for the estimation of
281 the optimal model parameters; and, ii) a cross-validation set Z_{crv} , used for the selection of the
282 optimal order of the model.

283 A further validation data set, Z_{val} , obtained collecting operating data from the normal, closed-
284 loop operation of the DSI system can be used for the assessment of the performance of the
285 trained model.

286 Denoting as $\hat{y}(t|\theta)$ the output prediction of the model, least-square method is used to
287 estimate the parameter vector θ^* that produces the best fit of the training data Z_{trn} :

$$288 \theta^* = \arg \min\{V(\theta, Z_{trn})\}, \quad \text{where } V(\theta, Z_{trn}) = \frac{1}{N_{trn}} \sum_{t=0}^{N_{trn}-1} (y(t) - \hat{y}(t|\theta))^2 \quad (6)$$

289 The cross-validation compares the performance of models with different orders, each with its
290 optimal parameter vector θ_i^* , estimated from the training set. The best model is the one for
291 which $V(\theta, Z_{crv})$ is the smallest. This procedure helps selecting a model structure without
292 unnecessary complexity (*i.e.* order), as excessively complex models tend to overfit the training
293 set and perform poorly in the cross-validation set. Lastly, the model with order and
294 parameters optimised for the Z_{trn} and Z_{crv} sets can be tested on the validation set Z_{val} and the
295 procedure can go on iteratively until a given threshold of performance is fulfilled.

296

297 **3.4 Virtual console**

298 The process model described in section 3.2 was integrated into a simulation environment,
299 where also the control loop and the other components of the DSI system were cloned as in

300 the real plant. The virtual console simulating the operation of the real DSI system consists of
301 four blocks, as shown in Figure 4.

302 The block “*Data import*” defines the inlet conditions of the simulation (inlet HCl concentration
303 and flue gas flowrate). These may be either actual plant data, collected at the measurement
304 point PM1 (see Fig. 1), or artificial data, created to test the system performance under specific
305 strain.

306 The input data of the “*Data Import*” block are then transferred to the “*DTS*” and “*DCS*” blocks.

307 The “*DTS*” block contains the process model described in section 3.2. The “*DCS*” block
308 simulates the control system described in section 2.2. Specifically, given as input signals the
309 HCl load at the inlet of the DTS (provided by the “*Data Import*” block) and the HCl load at the
310 outlet of the dry treatment system (modelled by the “*DTS*” block), this block evaluates with a
311 clock time of 1 s the command input for the actuator that regulates the feed rate of Ca(OH)₂.

312 The “*Actuator*” block simulates the operation of the screw feeder installed in the real plant.

313 The virtual actuator receives a percentage command of rotational speed calculated by the
314 “*DCS*” block and transforms it into a molar feed rate of solid reactant to the “*DTS*” block,
315 following a linear relationship between percentage command and feed rate that is
316 characteristic of the real feeder. The response of the actuator was modelled as a first order
317 transfer function:

318

$$319 \quad G(s) = \frac{R}{T_m \cdot s + 1} \quad (7)$$

320

321 where T_m is the actuation time of the screw feeder and R is the command to feed rate ratio.

322 This console allows the comparative testing of the behaviour of the DSI system under the
323 default control (section 2.2) or an alternative control, as discussed in the test case described
324 in section 4.

325

326 **3.5 Performance indicators selected to test alternative control strategies**

327 Both conventional indicators for process control performance and specific indicators
328 capturing the environmental and economic performance of the process were defined to allow
329 a comparison of alternative control strategies. The indicators are reported in Table 1
330 alongside their values obtained for the test case that will be introduced in section 4.

331 With respect to conventional process control indicators, these address the stability of the
332 output variables. The *instability of reactant injection*, expressed as the ratio of the CV of
333 reactant injection to the CV of inlet HCl mass flow, measures the time variability of the feed
334 rate of reactant imposed by the control system. All things equal, a control demanding less
335 variable feed rates is preferred as it induces less mechanical stress on the feeding system. The
336 *instability of HCl outlet*, expressed as the ratio of the CV of outlet HCl mass flow to the CV of
337 inlet HCl mass flow, measures the variability of the HCl mass flow at the outlet of the DSI
338 system.

339 Environmental indicators trace the material streams responsible for the indirect
340 environmental burdens of HCl removal: the *specific consumption of reactant*, expressed as
341 mass of reactant injected per mass of removed HCl, and the *specific generation of residues*,
342 expressed as mass of process residues generated per mass of removed HCl. These indicators
343 were monitored both for the Ca-based 1st stage and the bicarbonate-fed 2nd stage of HCl
344 removal, as the stabilisation of control in the 1st stage (object of the study) can also result in
345 a more stable operation for the 2nd stage. Therefore, an indicator of *overall generation of*

346 *residues*, encompassing both treatment stages, was also considered to have a complete
347 picture of the environmental benefit of control optimisation.

348 Lastly, an indicator addressing *overall operating costs* was also estimated, by translating the
349 streams of reactants and residues in operating costs considering their unit costs (see Table
350 S1).

351

352 **4 Test Case**

353

354 **4.1 Definition of the test case**

355 The test facility described in section 2.1 was used to define a test case for the application of
356 the methodology outlined in section 3. An open-loop test-run was used for the calibration of
357 the ARX model, while the accuracy of the resulting virtual console in reproducing the system
358 behaviour under its default control was assessed using several datasets available for the
359 normal operation of the DSI system. An example of alternative control was proposed, tuned
360 in the virtual console, then tested by full-scale test-runs on the real plant. The set of indicators
361 defined in section 3.4 was adopted to quantify the improvements in the stability of process
362 control and the economic and environmental performance.

363

364 **4.2 Calibration of the model and validation of the simulation for the test case**

365 The behaviour of the DSI system of the test facility was studied via step-response tests (Liu
366 and Gao, 2012). Input excitations were applied to the system by varying stepwise the feed
367 rate of $\text{Ca}(\text{OH})_2$. The effect on system behaviour was recorded by continuous monitoring (30
368 s resolution time) of the outlet HCl concentration (measurement point PM2 in Fig. 1), while
369 the inlet HCl concentration was also recorded (measurement point PM1 in Fig. 1).

370 On the basis of the discussion provided in section 3.2, the ARX model was calibrated
 371 considering the molar flowrate of inlet HCl (calculated from the measured inlet HCl
 372 concentration and inlet flue gas flowrate) and the feed rate of Ca(OH)₂ as input variables,
 373 while the molar flowrate of outlet HCl (product of the measured outlet HCl concentration
 374 and outlet flue gas flowrate) is the modelled output.

375 The virtual console including the calibrated process model was then validated, comparing its
 376 simulated outlet of HCl with the measured values in four datasets of operation of the DSI
 377 system under the reference control, provided the same input data (see section 5.1). The
 378 simulation error was quantitatively assessed by calculating a cumulative normalised root
 379 mean squared error (RMSE):

$$380 \text{ Normalised RMSE } (t) = \frac{\sqrt{\frac{1}{n(t)} \sum_{i=1}^{n(t)} (y_i - \hat{y}_i)^2}}{\frac{\sum_{i=1}^{n(t)} y_i}{n(t)}} \quad (8)$$

381 where $n(t)$ is the number of measurements/model evaluations at a given time.

382

383 **4.3 Selection and tuning of an alternative control**

384 Once the accuracy of the simulation results was demonstrated, the virtual console was used
 385 to test alternative approaches to the control of HCl removal operation. In this test case, the
 386 control logic described in section 2.2 (named in the following as “conventional control”) was
 387 substituted with a simple feedback control (named in the following as “alternative control”).
 388 Recalling Fig. 2, the conventional control is built to suppress any overrun of the setpoint of
 389 outlet HCl concentration with a spike of Ca(OH)₂ feed. The consequences of such approach,
 390 as illustrated in section 2.3, are an excess consumption of Ca(OH)₂ and unstable inlet
 391 conditions for the 2nd HCl removal stage fed with NaHCO₃, which, again, lead typically to an

392 excess consumption of NaHCO_3 . Conversely, a properly tuned control in purely feedback
393 action could limit the variability of both reactant feed and outlet HCl concentration.

394 The proposed feedback control is a simple proportional integral (PI) control. As the HCl inlet
395 concentration signal is by nature highly variable and vulnerable to noise contamination
396 (Coleman et al., 2019), the introduction of a derivative (D) control term was avoided, as it
397 could generate system instability (Ting et al., 2008).

398 Hence, in the simulation the two parameters of the feedback control, K_p gain and τ_I integral
399 time, were tuned. The values of the optimised parameters were $K_p = 2$ and $\tau_I = 345$ s.

400

401 **4.4 Performance assessment of the new control at the real plant**

402 Eventually, a comparative assessment of the performance of the conventional and alternative
403 control was carried out at the test facility. The alternative control was easily implemented, by
404 deactivating the feedforward control and updating the feedback settings to the tuned
405 parameters.

406 The test consisted in comparing a period of DSI process operation with the alternative control
407 with a period of operation with the conventional control. The HCl load released by waste
408 combustion can vary widely over time, and any control logic would manage better a low and
409 uniform inlet mass flow of HCl, rather than a high and fluctuating one. Thus, to ensure a
410 proper comparison, a period of operation experiencing an almost equal inlet mass flow of HCl
411 to that present during the test of the alternative control was selected as representative of the
412 conventional control performance.

413 As a measure of variability of inlet HCl load, the coefficient of variation (CV) of the HCl mass
414 flow during the test period was estimated:

415

416 $CV = \frac{\sigma}{\mu}$ (9)

417

418 where σ and μ are respectively the standard deviation and the mean of the measurements of
419 inlet HCl mass flow during the period of study. It was also ensured that the two periods of DSI
420 operation used for the comparison exhibited a similar CV of HCl mass flow, as it will be
421 discussed in section 5.3. The HCl removal efficiency X was also calculated as follows:

422 $X = \frac{\dot{m}_{HCl,in} - \dot{m}_{HCl,out}}{\dot{m}_{HCl,in}}$ (10)

423 The comparison among the performance of the alternative control strategies was carried out
424 calculating the indicators discussed in section 3.5.

425

426 5 Results and Discussion

427 5.1 Results of the validation of the simulation

428 Figure 5 reports the performance of the virtual console in simulating the behaviour of the
429 conventional process control of the DSI system on a sample dataset (other samples are shown
430 in Figures S1-S3 in the Supporting Information, SI). The percentage command to reactant feed
431 given by the real system and by the simulation are compared in Fig. 5a. Figure 5b compares
432 the measured and the simulated outlet HCl mass flow. The yellow curve represents the set
433 value of outlet HCl mass flow, which is a fluctuating value as it is defined as the product of the
434 fixed setpoint of outlet HCl concentration (see e.g. Fig. 2b) and the variable value of the flue
435 gas flowrate (see e.g. Fig. 2d). Again, it can be noticed that the conventional control treats the
436 set value more like a threshold than a setpoint, as discussed in section 2.3. Figure 5c plots the
437 cumulative average error of the simulation, represented as a normalised RMSE (introduced
438 in section 4.2). The error increases over time, indicating a loss of performance of the process

439 model nested in the simulation, that is typical of error accumulation in models of
440 autoregressive nature (Bazghaleh et al., 2013; Nelles, 2020). As evidenced also by the figures
441 in the SI, the error grows faster when outlet HCl fluctuates widely, while it remains almost
442 unchanged and may even decrease during periods of stable operation. It is clear that a simple
443 ARX model, linear by nature, falls short of achieving an accurate instantaneous prediction of
444 HCl outlet, which is the result of a complex and non-linear process involving gas-solid
445 reactions both in duct and on filter bags. Nonetheless, the simulation captures the average
446 system behaviour with acceptable resolution for the objective of the study.

447

448 **5.2 Results of the virtual testing of the alternative control**

449 The simulation was used for the tuning and for the virtual testing of the alternative PI control.
450 The tuning of the alternative control by the methodology outlined in section 4.3 provided the
451 following value for the control parameters: proportional gain $K_p = 2$ and integral time τ_I of
452 345 s. It should be recalled that the PI settings of the feedback component of the conventional
453 control (see section 2.2) are $K_p = 5$ and $\tau_I = 8$ s. The alternative control is less aggressive,
454 with a reduced proportional action and a significantly higher integral time, which lowers the
455 sensitivity of the control action to temporary deviations of the inlet HCl load. Figure 6a
456 illustrates the different behaviour of the alternative control strategy compared to the
457 conventional process control, on a data sample of 100 min. The simulation of the alternative
458 control was started during a significant deviation of the measured HCl outlet concentration
459 from the set-point value to emphasise the different mode of operation of the two control
460 strategies. The feed rate variations imposed by the alternative control strategy are markedly
461 smoother than those of the conventional control. The proposed strategy accepts momentary
462 upticks in the HCl outlet concentration, whereas the action of the original control results in

463 spikes of reactant feed. Conversely, the alternative control strategy imposes a slightly higher
464 feed rate than the original control during periods in which the latter operates in the
465 feedforward mode. These opposite behaviours are evident from the plot of cumulated
466 reactant consumption reported in Fig. 6c. Given that the variability of the reactant feed rate
467 has been highlighted in section 2.3 as one of the main causes of inefficient reactant
468 exploitation in the DTS, the alternative control strategy appears well suited to rationalise the
469 use of the reactant, thus minimising the resulting generation of process residues.

470

471 **5.3 Results of the field test of the alternative control**

472 The alternative PI control was implemented in the DCS of the test facility. As outlined in
473 section 4.4, a test run of the new control was carried out and the resulting operational data
474 were compared with a previous period under the conventional process control configuration.
475 The equivalence of action between the two controls was guaranteed by selecting the average
476 value of outlet HCl concentration in the previous day under the conventional control as the
477 setpoint for the test of the alternative control (see Fig. 7b).

478 Two 5-hour data samples with similar inlet flue gas conditions were selected for the
479 comparative assessment. The two time series are shown in Fig. 7a, where it is possible to
480 compare qualitatively the behaviour of the two control strategies, i.e. the feed rate of
481 reactant and the outlet HCl flowrate, depending on the inlet HCl flowrate. The relative
482 performance of the two controls was tracked via the indicators introduced in section 3.5.
483 Table 1 provides the list of the indicators used and the specific values obtained, while Figure
484 7c shows a radar plot comparing the normalised values of the performance indicators of the
485 alternative control to the reference one. Internal normalisation was used to obtain the values
486 shown in the figure. Given the low inlet SO₂ concentrations measured at the plant (in the

487 range 10 – 30 mg/Nm³) and the relatively low reactivity compared to HCl, the effect of SO₂ on
488 system performance is negligible and not discussed in the analysis.

489 First of all, the two 5-hour data samples present highly comparable inlet HCl loads, hence the
490 two controls are tested in a situation of similar stress. As reported in Table 1, the average inlet
491 HCl mass flow rate in the two periods is equal and its CV is 68% higher during the test of the
492 alternative control, i.e. the selection of data samples is slightly biased in favour of the
493 conventional control.

494 Figure 7 shows that the real behaviour of the proposed PI-only control is in line with what was
495 expected from the virtual simulation (see Fig. 6). The feed rate varies smoothly, with slow
496 corrections in face of any sharp variation in the outlet HCl flow. Conversely, the conventional
497 control reacts aggressively to deviations in the HCl outlet, with the characteristic spikes of
498 reactant feed rate already described in Fig. 2.

499 When the performance indicators introduced in section 3.5 are considered, the parameter
500 instability of reactant injection captures numerically this difference: while the commanded
501 feed rate of the original control shows a CV that is 4.3 times higher than the CV of the inlet
502 HCl molar flow, the CV of the commanded feed rate of the proposed control is only 1.24 times
503 higher (a 71% reduction, see Table 1).

504 At the same time, the specific consumption of reactant in the Ca(OH)₂-fed treatment stage is
505 11% lower with the proposed control. This confirms that the lower aggressivity of the new
506 control settings is not detrimental to the HCl removal efficiency of the system. On the
507 contrary, in the test period, the proposed control managed to achieve the desired HCl
508 removal performance with a significantly lower variability of reactant feed rate, which has the
509 further advantage of reducing the mechanical stress to the screw feeder and the reactant
510 transport system.

511 Another relevant metric is the instability of the outlet HCl flow, defined in section 3.5 as the
512 ratio between the CVs of outlet and inlet HCl molar flow. The proposed PI-only control
513 achieves a 39% reduction in this indicator. This means that the HCl load exiting the $\text{Ca}(\text{OH})_2$ -
514 fed treatment stage is less variable in time, thus the downstream NaHCO_3 -fed stage operates
515 on a less variable HCl inlet and is put in less stressful working conditions. As a consequence,
516 the optimisation of the control in the $\text{Ca}(\text{OH})_2$ stage generates also a 26% reduction in the
517 specific consumption of reactant in the subsequent NaHCO_3 stage (see again Table 1), whose
518 control was not modified.

519 The overall consequence of the increase in efficiency owing to the new PI-only control is the
520 reduction in the production of the solid process residues of HCl removal via both the gas-solid
521 reactions with $\text{Ca}(\text{OH})_2$ and NaHCO_3 . The new control achieves a 7% and a 22% reduction in
522 the generation of process residues, respectively in the 1st and 2nd treatment stages. The
523 overall effect is a 13% reduction of the amount of process waste generated by the HCl removal
524 operation. A further confirmation of this effect can be observed in figure S4 in the SI, which
525 shows the simulated action of the conventional control system considering the inlet HCl load
526 for the 5-hour dataset collected during the test-run. The figure evidences that the multiple
527 activations of the feedback mode would have caused a higher reactant consumption.

528

529 **5.4 Discussion**

530 In the light of the indicators in Table 1, the alternative control strategy tuned in the virtual
531 simulation was demonstrated to improve the overall economic and environmental
532 performance of the system. The consumption of reactants and the generation of process
533 residues were lowered in both the treatment stages, by increasing the efficiency of reactant
534 delivery. It was thus demonstrated that the main drawback of dry acid gas removal, i.e. the

535 required high excess of reactant, can be partially mitigated by introducing specific process
536 control strategies. In particular, for a multistage system as that of the test facility, it is worth
537 highlighting that an intervention limited to the 1st treatment stage can produce benefits also
538 on the 2nd stage, by enabling a more efficient operation thanks to the lowered variability of
539 the inlet HCl.

540 The alternative control strategy, based on a PI feedback control, however, has clear
541 limitations: even if the simple feedback action reduces the variability of HCl load compared
542 to the conventional control, the instability with respect to a setpoint is still quite high. More
543 advanced control strategies could offer further improvements. Nonetheless, the proposed
544 solution achieved the results in Table 1 with minimal need of full-scale testing and no
545 significant change in the control architecture of the system, demonstrating the ease of
546 implementation of better solid waste and reactant management via control optimisation.

547 The results obtained show that the procedure developed for the test of alternative control
548 strategies, based on a virtual console, and the metric introduced, based on the performance
549 indicators listed in Table 1, provide an effective approach to allow the improvement of the
550 environmental and economic operational performance of acid gas treatment systems.

551

552 6 Conclusions

553 With increasingly strict limits on the emission of airborne pollutants as HCl, the flue gas
554 treatment sections in WtE installations are experiencing problems of excessive consumption
555 of reactants and related high generation of solid residues destined to landfilling, which lead
556 to non-negligible indirect environmental burdens. By considering a reference state-of-the-art
557 acid gas removal system, the present study demonstrated that a standard process control

558 approach based exclusively on the suppression of HCl emissions might be a suboptimal
559 solution in terms of economic and environmental performance. A simple methodology based
560 on virtual simulation and limited full-scale test-runs allowed identifying and tuning an
561 alternative control strategy that achieved a reduction in the generation of solid process
562 residues equal to 7% in the optimised $\text{Ca}(\text{OH})_2$ -fed 1st stage of HCl removal and 13% in the
563 overall two-stage treatment line with respect to the original control configuration, while
564 maintaining the same HCl emission performance at stack.

565 Despite the relevant advantages in terms of reactant economy, a limitation of the proposed
566 solution is that it only partially alleviates the fluctuations in the HCl concentration at the outlet
567 of the 1st treatment stage, which are intrinsic to the WtE context. More advanced process
568 control strategies, taking into account process disturbances other than inlet pollutant
569 concentration and reactant feed rate, could be the key to develop plant-specific highly
570 performant model-based control schemes. However, the present study evidenced that
571 process control optimisation is a promising area of improvement in the management of WtE
572 flue gas treatment, not only to improve stable operation, but also to increase significantly the
573 economic and environmental performance of DSI processes without hindering the
574 compliance to emission limits at stack.

575

576 References

- 577 Akinola, T.E., Oko, E., Gu, Y., Wei, H.-L., Wang, M., 2019. Non-linear system identification
578 of solvent-based post-combustion CO₂ capture process. *Fuel* 239, 1213-1223.
- 579 Antonioni, G., Dal Pozzo, A., Guglielmi, D., Tugnoli, A., Cozzani, V., 2016. Enhanced
580 modelling of heterogeneous gas-solid reactions in acid gas removal dry processes. *Chem.*
581 *Eng. Sci.* 148, 140-154.
- 582 Ardolino, F., Boccia, C., Arena, U., 2020. Environmental performances of a modern waste-
583 to-energy unit in the light of the 2019 BREF document. *Waste Manage.* 104, 94-103.
- 584 Arena, U., 2015. From waste-to-energy to waste-to-resources: The new role of thermal
585 treatments of solid waste in the Recycling Society. *Waste Manage.* 37, 1-2.
- 586 Bagheri, M., Esfilar, R., Golchi, M.S., Kennedy, C.A., 2020. Towards a circular economy: A
587 comprehensive study of higher heat values and emission potential of various municipal
588 solid wastes. *Waste Manage.* 101, 210-221.
- 589 Bal, M., Reddy, T.T., Meikap, B.C., 2019. Removal of HCl gas from off gases using self-
590 priming venturi scrubber. *J. Haz. Mat.* 364, 406-418.
- 591 Bazghaleh, M., Mohammadzaheri, M., Grainger, S., Cazzolato, B., Lu, T.-F., 2013. A new
592 hybrid method for sensorless control of piezoelectric actuators. *Sensors and Actuators A:*
593 *Physical* 194, 25-30.
- 594 Beylot, A., Hochar, A., Michel, P., Descat, M., Ménard, Y., Villeneuve, J., 2018. Municipal
595 Solid Waste Incineration in France: An Overview of Air Pollution Control Techniques,
596 Emissions, and Energy Efficiency. *J. Ind. Ecol.* 22, 1016-1026.
- 597 Bogush, A., Stegemann, J.A., Wood, I., Roy, A., 2015. Element composition and
598 mineralogical characterisation of air pollution control residue from UK energy-from-waste
599 facilities. *Waste Manage.* 36, 119-129.
- 600 CEN, 2019. CEN/TS 17337:2019 – Stationary source emissions - Determination of mass
601 concentration of multiple gaseous species - Fourier transform infrared spectroscopy.
602 European Committee for Standardization, Bruxelles, Belgium.
- 603 Choi, S., Yoo, C., Lee, I.-B., 2002. SO_x monitoring and neural net classification in the power
604 plant. *J. Environ. Eng.* 128, 911-918.
- 605 Cignitti, S., Mansouri, S.S., Sales-Cruz, M., Jensen, F., Huusom, J.K., 2016. Dynamic
606 Modeling and Analysis of an Industrial Gas Suspension Absorber for Flue Gas
607 Desulfurization. *Emiss. Control Sci. Technol.* 2, 20-32.
- 608 Coleman, M.D., Ellison, M., Robinson, R.A., Gardiner, T.D., Smith, T.O.M., 2019.
609 Uncertainty requirements of the European Union’s Industrial Emissions Directive for
610 monitoring sulfur dioxide emissions: Implications from a blind comparison of sulfate
611 measurements by accredited laboratories. *J. Air Waste Manage. Assoc.* 69, 1070-1078.
- 612 Dal Pozzo, A., Moricone, R., Tugnoli, A., Cozzani, V., 2019. Experimental Investigation of
613 the Reactivity of Sodium Bicarbonate toward Hydrogen Chloride and Sulfur Dioxide at Low
614 Temperatures. *Ind. Eng. Chem. Res.* 58, 6316-6324.

615 Dal Pozzo, A., Lazazzara, L., Antonioni, G., Cozzani, V., 2020. Techno-economic
616 performance of HCl and SO₂ removal in waste-to-energy plants by furnace direct sorbent
617 injection. *J. Haz. Mat.* 394, 122518.

618 Dal Pozzo, A., Guglielmi, D., Antonioni, G., Tugnoli, A., 2018a. Environmental and
619 economic performance assessment of alternative acid gas removal technologies for
620 waste-to-energy plants. *Sust. Prod. Consumption* 16, 202-215.

621 Dal Pozzo, A., Armutlulu, A., Rekhtina, M., Müller, C.R., Cozzani, V. 2018b. CO₂ Uptake
622 Potential of Ca-Based Air Pollution Control Residues over Repeated Carbonation-
623 Calcination Cycles. *Energy Fuels* 32, 5386-5395.

624 Dal Pozzo, A., Giannella, M., Antonioni, G., Cozzani, V., 2018c. Optimization of the
625 economic and environmental profile of HCl removal in a municipal solid waste incinerator
626 through historical data analysis. *Chem. Eng. Trans.* 67, 463-468.

627 Dal Pozzo, A., Guglielmi, D., Antonioni, G., Tugnoli, A., 2017. Sustainability analysis of dry
628 treatment technologies for acid gas removal in waste-to-energy plants. *J. Clean. Prod.* 162,
629 1061-1074.

630 Dal Pozzo, A., Antonioni, G., Guglielmi, D., Stramigioli, C., Cozzani, V., 2016. Comparison
631 of alternative flue gas dry treatment technologies in waste-to-energy processes. *Waste*
632 *Manage.* 51, 81-90.

633 Damgaard, A., Riber, C., Fruergaard, T., Hulgaard, T., Christensen, T.H., 2010. Life-cycle-
634 assessment of the historical development of air pollution control and energy recovery in
635 waste incineration. *Waste Manage.* 30, 1244-1250.

636 De Greef, J., Villani, K., Goethals, J., Van Belle, H., Van Caneghem, J., Vandecasteele, C.,
637 2013. Optimising energy recovery and use of chemicals, resources and materials in
638 modern waste-to-energy plants. *Waste Manage.* 33, 2416-2424.

639 Dong, J., Jeswani, H.K., Nzihou, A., Azapagic, A., 2020. The environmental cost of
640 recovering energy from municipal solid waste. *Appl. Energy* 267, 114792.

641 Ephraim, A., Ngo, L.D., Pham Minh, D., Lebonnois, D., Peregrina, C., Sharrock, P., Nzihou,
642 A., 2019. Valorization of Waste-Derived Inorganic Sorbents for the Removal of HCl in
643 Syngas. *Waste Biomass Valorization* 10, 3435-3446.

644 Foo, R., Berger, R., Heiszwolf, J.J., 2016. Reaction Kinetic Modeling of DSI for MATS
645 Compliance. In: Proceedings of the Power Plant Pollutant Control and Carbon
646 Management "MEGA" Symposium, Baltimore, MD, USA, 16–19 August 2016

647 Gassner, M., Nilsson, J., Nilsson, E., Palmé, T., Züfle, H., Bernero, S., 2014. A data-driven
648 approach for analysing the operational behaviour and performance of an industrial flue
649 gas desulphurisation process. *Computer Aided Chem. Eng.* 33, 661-666.

650 Gerassimidou, S., Velis, C.A., Williams, P.T., Castaldi, M.J., Black, L., Komilis, D., 2020.
651 Chlorine in waste-derived solid recovered fuel (SRF), co-combusted in cement kilns: A
652 systematic review of sources, reactions, fate and implications. *Critical Reviews in*
653 *Environmental Science and Technology*, in press.

654 Goodall, P.; Sharpe, R.; West, A., 2019. A data-driven simulation to support
655 remanufacturing operations. *Computers in Industry* 105, 48-60.

656 Guo, Y., Xu, Z., Zheng, C., Shu, J., Dong, H., Zhang, Y., Weng, W., Gao, X., 2019. Modeling
657 and optimization of wet flue gas desulfurization system based on a hybrid modeling
658 method. *J. Air Waste Manage. Assoc.* 69, 565-575.

659 Gutiérrez Ortiz, F.J., Ollero, P., 2008. A realistic approach to modeling an in-duct
660 desulfurization process based on an experimental pilot plant study. *Chem. Eng. J.* 141,
661 141-150.

662 Harriott, P., 1990. A Simple Model for SO₂ Removal in the Duct Injection Process. *J. Air
663 Waste Manage. Assoc.* 40, 998-1003.

664 Hartman, M., Svoboda, K., Pohorely, M., Syc, M., 2013. Thermal Decomposition of Sodium
665 Hydrogen Carbonate and Textural Features of Its Calcines. *Ind. Eng. Chem. Res.* 52, 10619-
666 10626.

667 Hunt, G., Sewell, M., 2015. Utilizing Dry Sorbent Injection Technology to Improve Acid Gas
668 Control. In: 34th International Conference on Thermal Treatment Technologies &
669 Hazardous Waste Combustors, Houston, TX, USA, 20-22 October 2015

670 Iizuka, A., Morishita, Y., Shibata, E., Takatoh, C., Cho, H., 2020. Basic Study of the Reaction
671 of Calcium Hydroxide with Hydrogen Chloride Using Single Crystals. *Ind. Eng. Chem. Res.*
672 59, 9699-9704.

673 Kameda, T., Tochinai, M., Kumagai, S., Yoshioka, T., 2020. Treatment of HCl gas by cyclic
674 use of Mg–Al layered double hydroxide intercalated with CO₃²⁻. *Atmospheric Pollution
675 Res.* 11, 290-295.

676 Kim, K.-D., Jeon, S.-M., Hasolli, N., Lee, K.-S., Lee, J.-R., Han, J.-W., Kim, H.T., Park, Y.-O.,
677 2017. HCl removal characteristics of calcium hydroxide at the dry-type sorbent reaction
678 accelerator using municipal waste incinerator flue gas at a real site. *Korean J Chem Eng*
679 34, 747-756.

680 Kockmann, N., 2019. Digital methods and tools for chemical equipment and plants.
681 *Reaction Chemistry and Engineering* 4, 1522-1529.

682 Lausset, C., Cherubini, F., del Alamo Serrano, G., Becidan, M., Strømman, A.H., 2016.
683 Life-cycle assessment of a Waste-to-Energy plant in central Norway: Current situation and
684 effects of changes in waste fraction composition. *Waste Manage.* 58, 191-201.

685 Liu, T., Gao, F., 2012. Step Response Identification of Stable Processes. In: Liu, T., Gao, F.,
686 *Industrial Process Identification and Control Design*, Springer-Verlag London, London, UK.

687 Liu, S., Sun, L., Zhu, S., (...), Chen, X., Zhong, W., 2020. Operation strategy optimization of
688 desulfurization system based on data mining. *Appl. Mathematical Modelling* 81, 144-158.

689 Ljung, L., 2010. Perspectives on system identification. *Annual Reviews in Control* 34, 1-12.

690 Margallo, M., Taddei, M.B.M., Hernández-Pellón, A., Aldaco, R., Irabien, A., 2015.
691 Environmental sustainability assessment of the management of municipal solid waste
692 incineration residues: A review of the current situation. *Clean Technol. Environ. Policy* 17,
693 1333-1353.

694 Montagnaro, F., Balsamo, M., Salatino, P., 2016. A single particle model of lime sulphation
695 with a fractal formulation of product layer diffusion. *Chem. Eng. Sci.* 156, 115-120.

696 Muratori, G., Dal Pozzo, A., Antonioni, G., Cozzani, V., 2020. Application of Multivariate
697 Statistical Methods to the Modelling of a Flue Gas Treatment Stage in a Waste-to-energy
698 Plant. *Chem. Eng. Trans.* 82, 397-402.

699 Nelles, O., 2020. Nonlinear System Identification: From Classical Approaches to Neural
700 Networks, Fuzzy Models, and Gaussian Processes. Springer Nature, Berlin, Germany.

701 Neuwahl, F., Cusano, G., Gomez Benavides, J., Holbrook, S., Roudier, S., 2019. Best
702 Available Techniques (BAT) Reference Document for Waste Incineration. EUR 29971 EN.
703 doi:10.2760/761437

704 Ouda, O.K.M., Raza, S.A., Nizami, A.S., Rehan, M., Al-Waked, R., Korres, N.E., 2016. Waste
705 to energy potential: A case study of Saudi Arabia. *Renewable Sustainable Energy Reviews*
706 61, 328-340.

707 Peng, H., Ozaki, T., Toyoda, Y., Shioya, H., Nakano, K., Haggan-Ozaki, V., Mori, M., 2004.
708 RBF-ARX model-based nonlinear system modeling and predictive control with application
709 to a NO_x decomposition process. *Control Engineering Practice* 12, 191-203.

710 Quina, M.J., Bontempi, E., Bogush, A., Schlumberger, S., Weibel, G., Braga, R., Funari, V.,
711 Hyks, J., Rasmussen, E., Lederer, J., 2018. Technologies for the management of MSW
712 incineration ashes from gas cleaning: New perspectives on recovery of secondary raw
713 materials and circular economy. *Sci. Total Environ.* 635, 526-542.

714 Saleem, M., Krammer, G., 2012. On the Stability of Pulse-Jet Regenerated-Bag Filter
715 Operation. *Chemical Engineering and Technology* 35, 877-884.

716 Smrekar, J., Potočnik, P., Senegačnik, A., 2013. Multi-step-ahead prediction of NO_x
717 emissions for a coal-based boiler. *Appl. Energy* 106, 89-99.

718 Ting, C.-H., Chen, H.-H., Yen, C.-C., 2008. A PID ratio control for removal of HCl/SO_x in flue
719 gas from refuse municipal incinerators. *Control Engineering Practice* 16, 286-293.

720 Van Caneghem, J., Van Acker, K., De Greef, J., Wauters, G., Vandecasteele, C., 2019.
721 Waste-to-energy is compatible and complementary with recycling in the circular
722 economy. *Clean Technol. Environ. Policy*, in press.

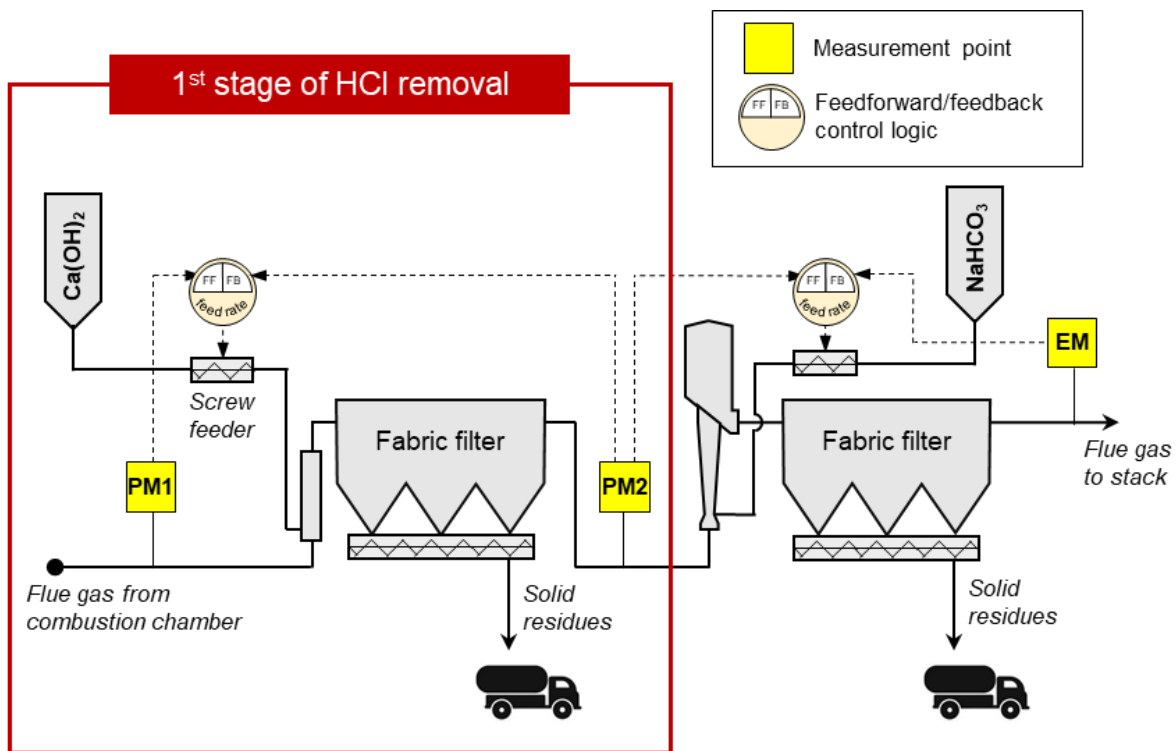
723 Vehlow, J., 2015. Air pollution control systems in WtE units: An overview. *Waste Manage.*
724 37, 58-74.

725 Wu, C., Kang, S.-J., Keener, T.C., Lee, S.-K., 2004. A model for dry sodium bicarbonate duct
726 injection flue gas desulfurization. *Advances in Environmental Research* 8, 655-666.

727 Yang, N., Damgaard, A., Scheutz, C., Shao, L.-M., He, P.-J., 2018. A comparison of chemical
728 MSW compositional data between China and Denmark. *J. Environ. Sci.* 74, 1-10.

729 Zhang, H., Yu, S., Shao, L., He, P., 2019. Estimating source strengths of HCl and SO₂
730 emissions in the flue gas from waste incineration. *J. Environ. Sci.* 75, 370-377.

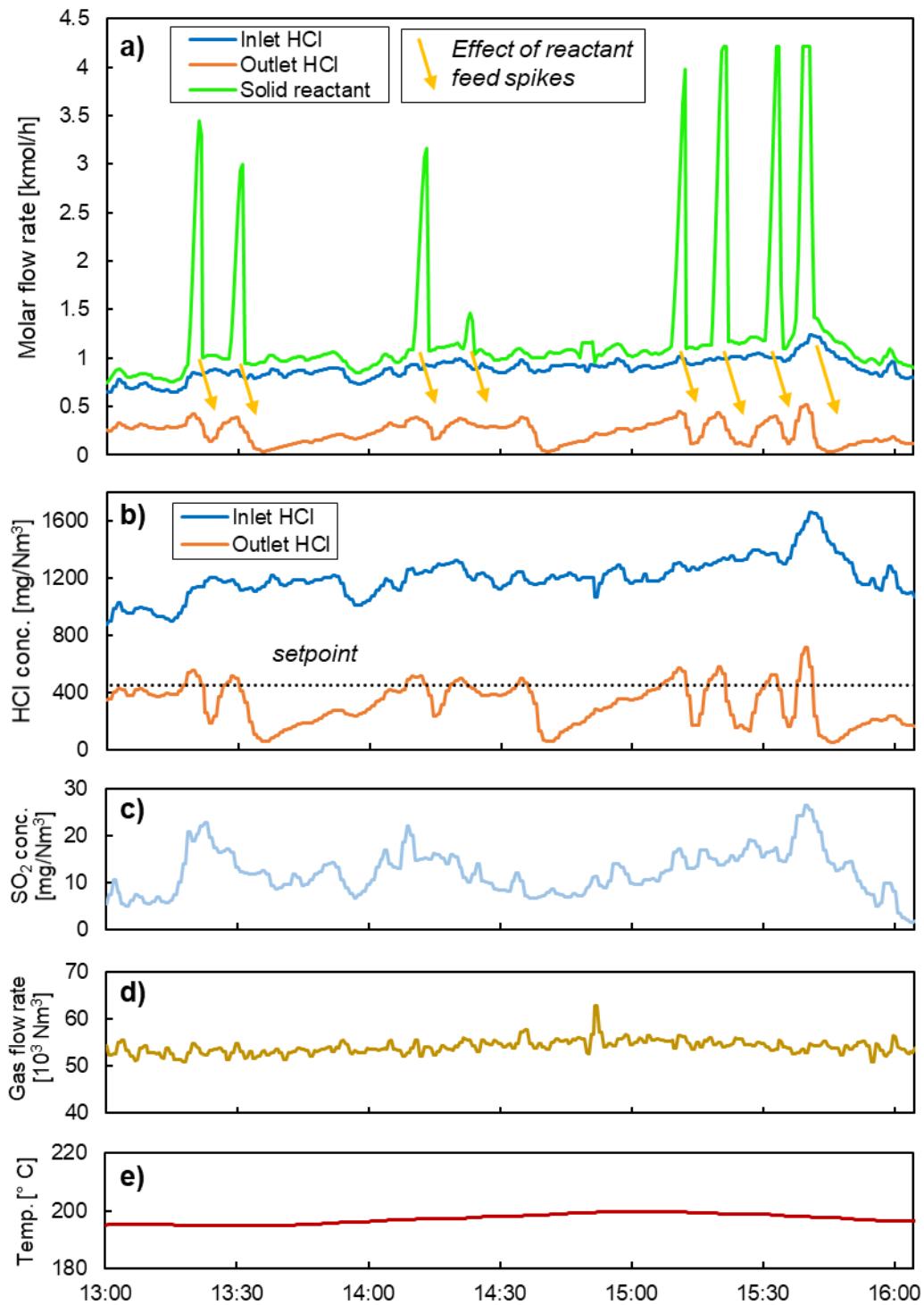
731
732
733
734
735



738

739 **Figure 1.** Scheme of the two-stage acid gas abatement system of the test facility considered,
740 including measurement points of flue gas composition (PM1, PM2 = process measurement,
741 EM = measurement at stack) and control loops for reactant feed rate. Control optimization of
742 1st stage (red box in the figure) was the object of the study.

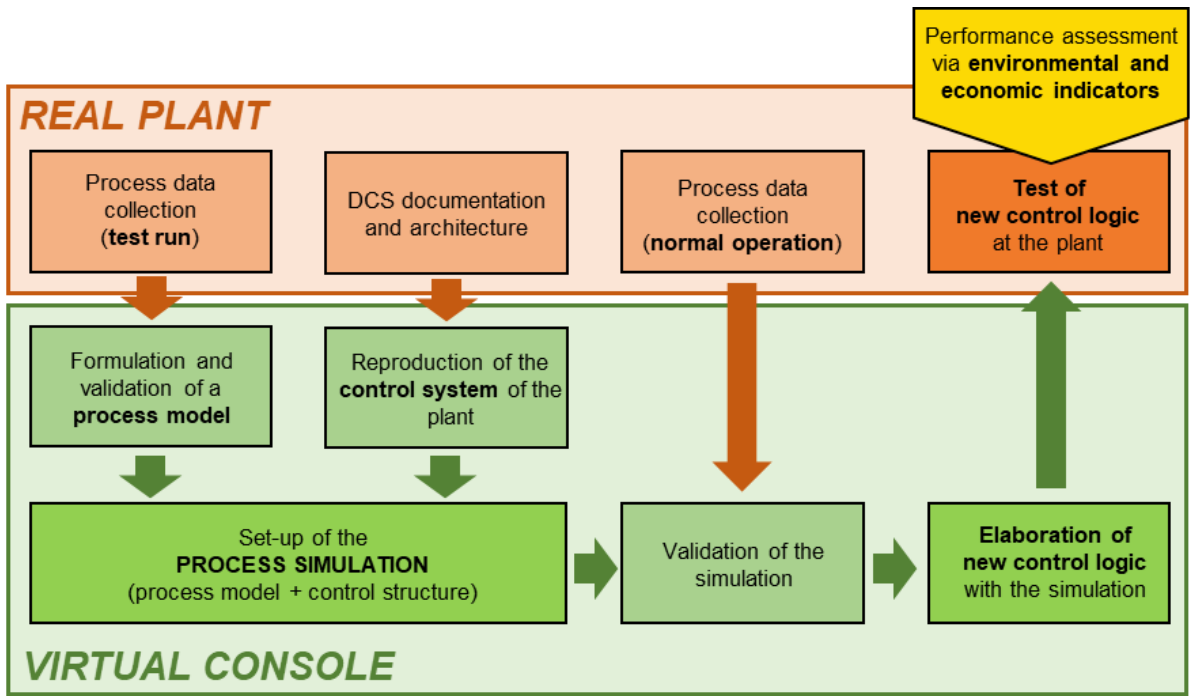
743



744

745 **Figure 2.** Data recorded by the distributed control system (DCS) of an Italian WtE facility
 746 showing: a) the typical trend of inlet and outlet HCl flowrate and solid reactant feed rate
 747 during normal operation of the 1st stage acid gas removal unit applying the conventional
 748 process control strategy; b) threshold setpoint with respect to HCl inlet and outlet
 749 concentrations; c) SO₂ concentration; d) flue gas flowrate; e) operating temperature.

750



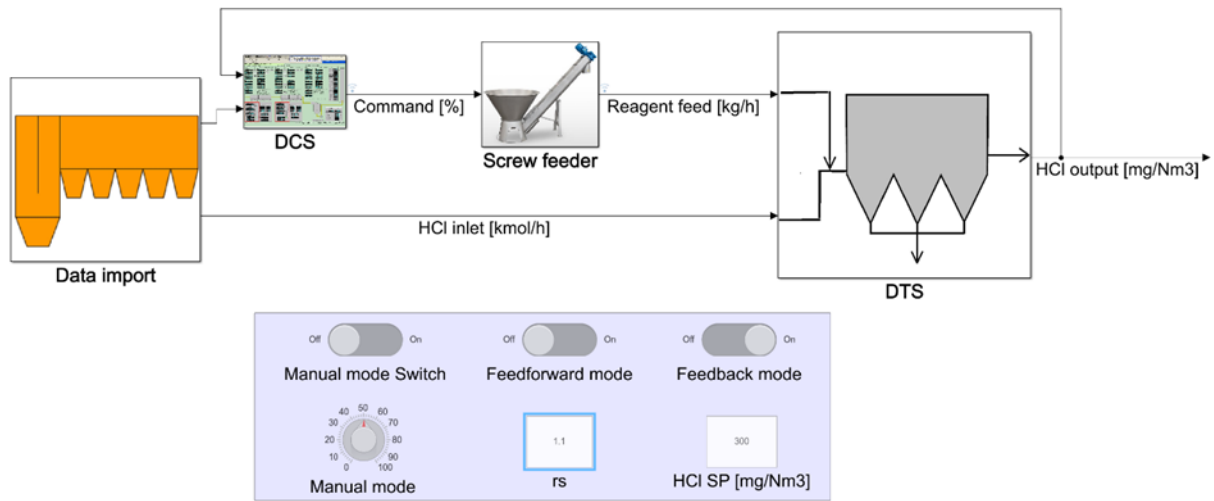
751

752 **Figure 3.** Methodology developed for testing and tuning of improved process control

753 strategies.

754

755

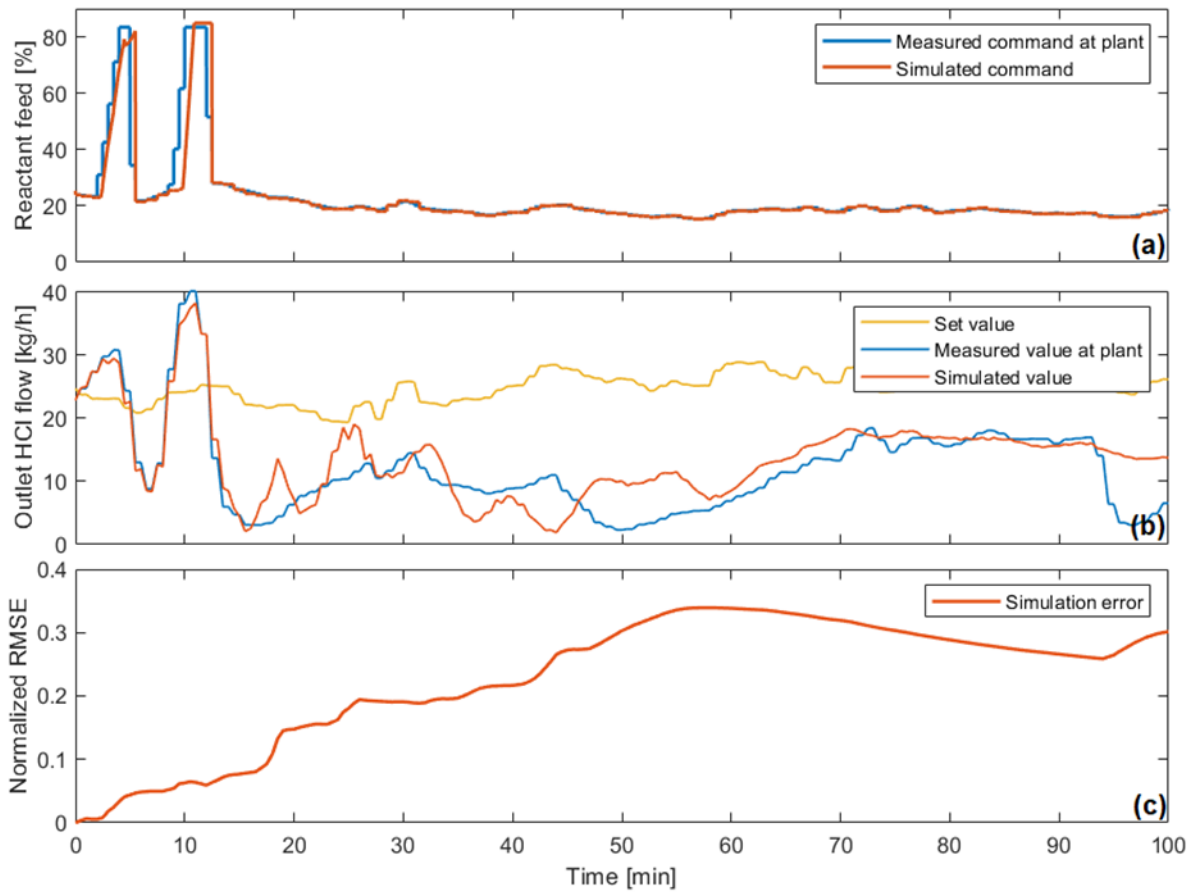


756

757 **Figure 4.** Virtual console developed to simulate the DSI process (1st stage of the acid gas

758 removal system in Fig. 1) using the Simulink[®] software tool.

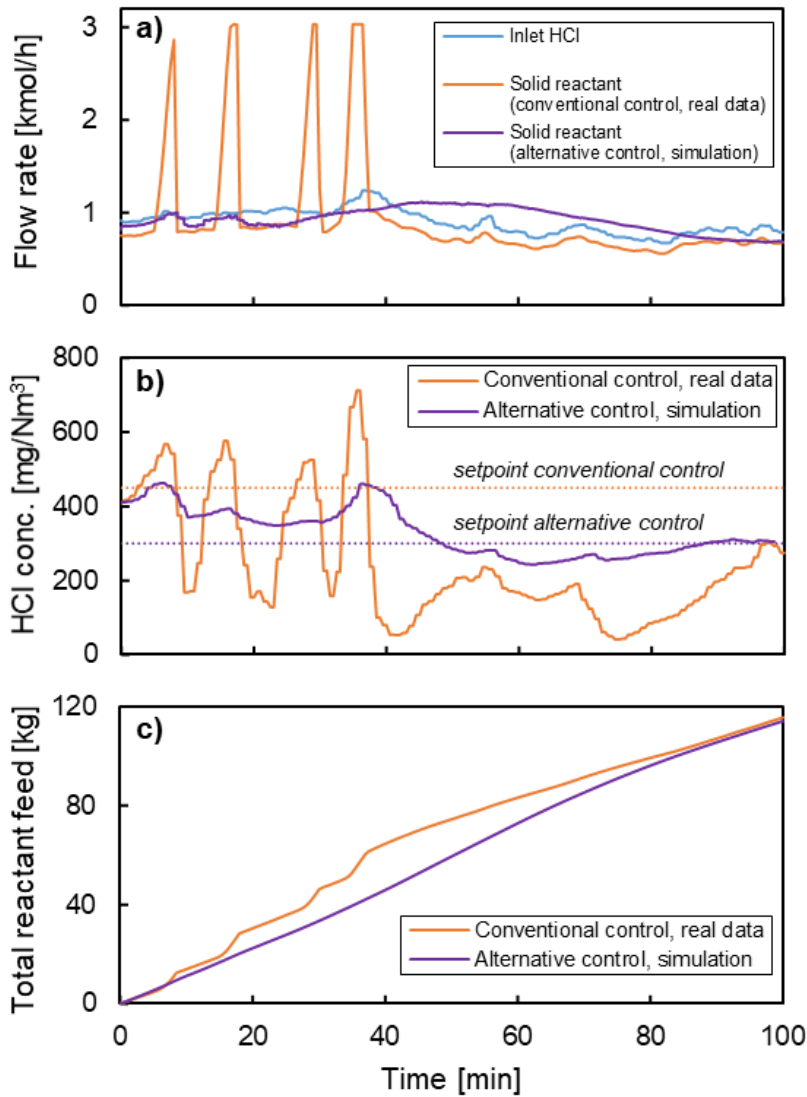
759



760
761

762 **Figure 5.** Performance of the virtual console in simulating the behaviour of the conventional
 763 control of the system: a) measured vs. simulated command of reactant feed, b) measured vs.
 764 simulated outlet HCl flow rate, compared to the set value of the control, c) cumulative average
 765 error of the simulation.

766



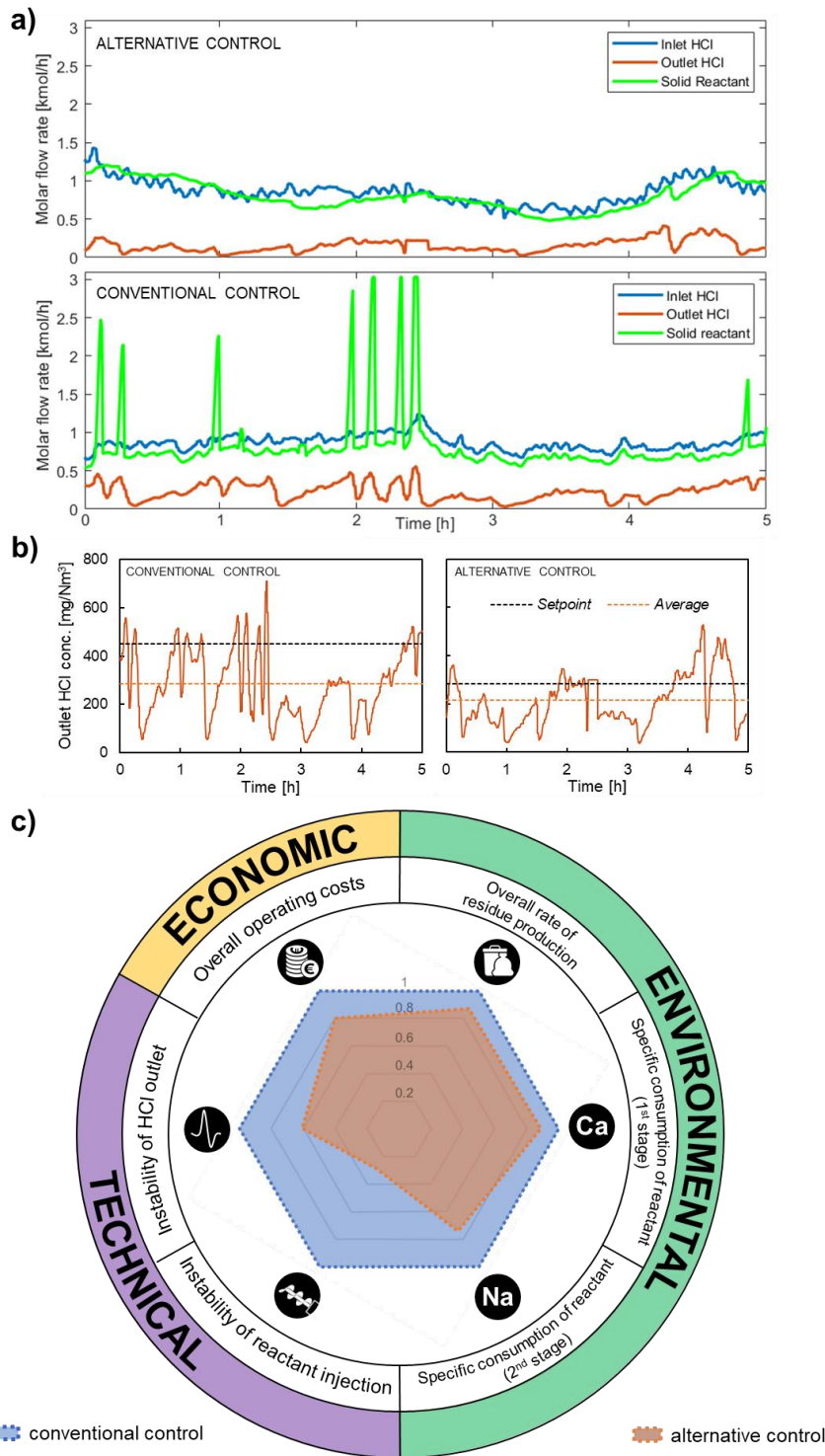
767

768 **Figure 6.** a) Simulation of the reactant feed rate by the alternative PI control strategy

769 compared to the conventional process control on a sample dataset; b) deviation of the outlet

770 HCl concentration from the respective setpoints, c) resulting cumulated reactant consumption.

771



778 **Table 1.** Performance of the alternative control strategy vs. the conventional process control
 779 monitored according to the performance indicators introduced in section 3.5.

Parameter or indicator		Test period		Δ
		Conventional control	Alternative control	
Inlet HCl mass flow rate (kg/h)	μ	64.4	64.4	-
	CV	0.12	0.19	+68%
Feed rate of reactant, Ca(OH) ₂ (kg/h)	μ	61.1	60.0	-2%
	CV	0.49	0.24	-52%
Outlet HCl mass flow rate (kg/h)	μ	17.2	12.5	-27%
	CV	0.51	0.52	+2%
HCl removal efficiency (%)	μ	75.8	82.3	+9%
	CV	11.2	8.5	-24%
Instability of reactant injection (CV of Ca(OH) ₂ feed rate / CV of inlet HCl)		4.27	1.24	-71%
Instability of HCl outlet (CV of outlet HCl / CV of inlet HCl)		4.4	2.7	-39%
Specific consumption of reactant (1 st stage) (kg of Ca(OH) ₂ fed / kg of HCl removed)		1.30	1.16	-11%
Specific generation of residues (1 st stage) (kg of residues / kg of HCl removed)		1.80	1.67	-7%
Specific consumption of reactant (2 nd stage) (kg of NaHCO ₃ fed / kg of HCl removed)		3.85	2.86	-26%
Specific generation of residues (2 nd stage) (kg of residues / kg of HCl removed)		2.55	2.00	-22%
Overall rate of residue production (kg of residues / kg of HCl removed)		2.00	1.73	-13%
Overall economic performance (€ of operating costs / kg of HCl removed)		1.86	1.48	-20%

780

781

1 Economic and environmental benefits by improved process control strategies in HCl removal
2 from waste-to-energy flue gas

3

4 *Alessandro Dal Pozzo, Giacomo Muratori, Giacomo Antonioni, Valerio Cozzani**

5 LISES - Dipartimento di Ingegneria Civile, Chimica, Ambientale e dei Materiali, Alma Mater
6 Studiorum - Università di Bologna, via Terracini n.28, 40131 Bologna, Italy

7

8 (*)*corresponding author*, Tel. +39-051-2090240, Fax +39-051-2090247, e-mail:
9 valerio.cozzani@unibo.it

10

11 **Abstract**

12 The control of HCl emission in waste-to-energy (WtE) facilities is a challenging flue gas
13 treatment problem: the release of HCl from waste combustion is highly variable in time and
14 the HCl emission standards are typically far lower in WtE than in any other industry.
15 Traditional process control approaches in dry HCl removal processes are generally based on
16 feeding a large excess of solid reactants to the system, to ensure robustness and a wide safety
17 margin in the compliance to environmental regulations. This results in the production of a
18 high amount of unreacted sorbents, strongly increasing the generation of solid wastes that
19 need to be disposed. In the present study, an approach was developed to allow the
20 implementation of improved control strategies for dry HCl abatement systems in operating
21 full-scale facilities. Its objective is the reduction of the reactant feed and the waste
22 production, while still providing an adequate safety margin for emission compliance. The
23 approach was based on the reproduction of the behaviour of the real system in a virtual
24 console that allows the extensive testing of alternative control strategies, limiting the need of
25 demanding test-runs at the real plant. A test case on an Italian WtE facility demonstrated the
26 capability of a control logic tuned in the virtual console to achieve a 13% reduction in the
27 consumption of reactants and generation of process residues, with unchanged HCl removal

28 **efficiency.** The results evidence the wide opportunities for optimisation of dry acid gas
29 removal systems, in particular when multistage systems are implemented.

30 **Keywords:** waste-to-energy, HCl, process optimization, dry sorbent injection.

31 1 Introduction

32 In a modern waste management system, waste-to-energy (WtE) facilities have the role to
33 divert from landfilling waste streams for which recycling is currently technically or
34 economically unfeasible (Nizami et al., 2016) and enabling their thermal valorisation (Arena
35 et al., 2015), thus facilitating the transition to a circular economy (Bagheri et al., 2020; Van
36 Caneghem et al., 2019). Thanks to increasingly ambitious environmental regulations, the
37 emission of several air pollutants related to WtE operation has been reduced more than
38 tenfold in the last decades (Ardolino et al., 2020; Damgaard et al., 2010). However, in the
39 current holistic approach to environmental protection, the reduction of impacts has to go
40 beyond the minimisation of the emission of pollutants at the stack of the plant. Also indirect
41 impacts, e.g. those associated to the consumption of reactants and the production of process
42 residues in the flue gas treatment system of the plant (Dal Pozzo et al., 2017; Dong et al.,
43 2020; Lousselet et al., 2016), needs to be minimised.

44 Hydrogen chloride (HCl) is a typical pollutant in WtE flue gases, arising from the combustion
45 of waste containing chlorine (Zhang et al., 2019). Chlorine is widely dispersed amongst organic
46 and inorganic compounds present in several waste items (Gerassimidou et al., 2020; Yang et
47 al., 2018). Among the different techniques available for HCl removal (Bal et al., 2019; Dal
48 Pozzo et al., 2019; Ephraim et al., 2019; Kameda et al., 2020), dry sorbent injection (DSI) is
49 one of the technologies more frequently implemented (Beylot et al., 2018; Dal Pozzo et al.,
50 2018a). DSI consists in the in-duct addition of an alkaline powdered reactant (e.g. calcium

51 hydroxide or sodium bicarbonate), which neutralises acid pollutants as HCl via gas-solid
52 reaction (Antonioni et al., 2016). DSI, adopted in either single or two-stage configurations (Dal
53 Pozzo et al., 2016; De Greef et al., 2013), is considered among the best available techniques
54 for flue gas treatment in WtE installations recommended by the European Union (Neuwahl et
55 al., 2019).

56 The main environmental drawback of DSI systems is the high stoichiometric excess of reactant
57 feed that is required to achieve high HCl removal efficiency (Vehlow, 2015). The resulting
58 excess consumption of reactant leads to the generation of relevant streams of solid **process**
59 **residues in the fabric filters, where they are collected together with fly ashes and**
60 **micropollutants. The presence of these other components in the collected process residues**
61 **causes the stream to be considered as hazardous waste and to require its disposal in**
62 **dedicated landfill sites (Dal Pozzo et al., 2018b; Kameda et al., 2020).**

63 **In addition, given that the composition of the waste burnt in the combustion chamber of a**
64 **WtE plant varies widely over time, the resulting extreme variability of HCl concentration at**
65 **the inlet of the flue gas treatment section (Dal Pozzo et al., 2020) is an inherent instability**
66 **that limits the effectiveness of conventional control strategies in calibrating the reactant feed**
67 **needed to maintain a constant concentration setpoint at the outlet. Thus, the prevailing trend**
68 **in control strategies is to calibrate the process control parameters of the DSI system on the**
69 **safe side, and even more so accept high excess feed rates of reactants to minimise the**
70 **possible occurrence of overruns of HCl emission limits at stack.**

71 **A more accurate setting of the DSI control system could ensure not only a safe compliance of**
72 **emission limits at stack, but also a reduction of the consumption of reactants and the**
73 **generation of process residues. These in principle represent an undesired environmental**

74 **burden shift between different compartments (from air to soil/water) (Bogush et al., 2015;**
75 **Margallo et al., 2015; Quina et al., 2018).**

76 The problem of the optimisation of flue gas treatment control with reference either to the
77 WtE context or to acid pollutants (HCl, SO₂, HF) is scarcely addressed in scholarly literature.
78 Ting et al. (2008) described the design of a PID control for acid gas removal via semi-dry
79 scrubbing in a WtE plant, with parameter tuning performed during commissioning operation.
80 Gassner et al. (2014) explored the use of data-driven modelling approaches to describe the
81 non-stationary operational behaviour of a semi-dry flue gas desulfurization process. Cignitti
82 et al. (2016) developed a simple first principle model to predict the dynamics of a semidry SO₂
83 absorber in desulfurization units of coal-fired power plants, while Guo et al. (2019) used a
84 hybrid approach, blending first principles and neural network, to model and optimise a wet
85 flue gas desulfurization unit. Yet, the focus of these recent studies has been mainly the
86 theoretical development of enhanced dynamic models of the process, rather than their
87 implementation in real control schemes. In particular, to the best of the authors' knowledge,
88 no previous paper addresses the potential environmental and economic advantages in terms
89 of reduced reactant consumption and related waste generation achievable with process
90 control optimisation in WtE acid gas removal.

91 Furthermore, control optimisation in the WtE context is made complex by the fact that
92 conventional direct tuning via extensive test runs during plant operation is generally
93 incompatible with the need to comply with strict HCl emission limits in presence of a highly
94 variable inlet load of HCl coming from waste combustion. In this regard, the set-up of data-
95 driven simulations of the real system in a virtual environment, as more and more frequently
96 performed in the manufacturing (Goodall et al., 2019) and process industry (Kockmann,
97 2019), could drastically reduce the need of field tests. By this strategy, the screening and the

98 tuning of new control settings is carried out directly in a virtual set-up, thus limiting the
99 number of in-field test runs only to those needed for the initial calibration of the simulation
100 and for the final trial of the new control system.

101 The present study focuses on the development of an approach for the optimisation of process
102 control in a typical DSI system for HCl removal based on a virtual environment. A dynamic
103 simulation of the dry treatment system was built in a virtual console implemented using the
104 Simulink software. A data-driven process model, calibrated with a specific set of test data,
105 nested into a reproduction of the control system of the DSI unit, was thus obtained and
106 validated. The virtual console was used to test and tune an alternative control strategy, with
107 the objective to reduce the stoichiometric excess of reactant associated to HCl removal. The
108 alternative control was then tested in full scale at the real plant, demonstrating the potential
109 for significant environmental and economic benefits deriving from the reduction in reactant
110 consumption and related process waste generation.

111

112 2 Reference system and test facility

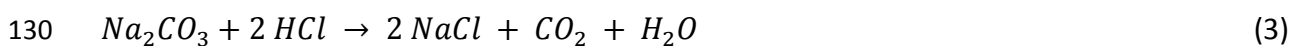
113

114 2.1 HCl removal system

115 The two-stage acid gas abatement system of a medium-sized (400 t/d of waste treated) WtE
116 facility located in Northern Italy was used as case study. As shown in Fig. 1, this system is
117 based on two consecutive steps of dry sorbent injection and filtration, taking place at ~180
118 °C, downstream of the heat recovery section of the plant. In the first stage, calcium hydroxide,
119 $\text{Ca}(\text{OH})_2$, is injected, triggering the following gas-solid reaction of HCl neutralisation (Iizuka et
120 al., 2020):



122 A fabric filter separates the solid product of reaction from the flue gas, together with a
123 relevant unreacted fraction of $\text{Ca}(\text{OH})_2$, present both due to the excess feed of reactant and
124 for the intrinsic diffusional limitations of gas-solid reaction (i.e. the phenomenon of
125 incomplete conversion discussed by Antonioni et al., 2016). In the second stage, the dry
126 injection is based on sodium bicarbonate, NaHCO_3 . At the injection temperature and, in
127 general, at $T > 130 \text{ }^\circ\text{C}$ (see Hartman et al., 2013), NaHCO_3 decomposes to porous sodium
128 carbonate (Na_2CO_3), which in turn absorbs HCl (Dal Pozzo et al., 2019):



131 Again, the solid product of reaction and an unreacted fraction of reactant are collected by a
132 fabric filter. This two-stage configuration is adopted in several European WtE installations and
133 it is appreciated for its built-in redundancy in terms of emission control (De Greef et al., 2013)
134 and its flexibility that allows different repartitions of abatement demand between the two
135 stages (Dal Pozzo et al., 2016).

136 As shown in Fig. 1, the present study is focused on the optimisation of the control of the
137 $\text{Ca}(\text{OH})_2$ 1st stage of acid gas removal, referred to in the following as dry sorbent injection (DSI)
138 system. As discussed in the following, the optimisation and tuning of the process control of
139 the 1st stage not only improves the performance of the stage, but, stabilising the HCl outlet
140 concentration, it also favours the optimal performance of the 2nd stage.

141

142 **2.2 Process control**

143 In the test facility, a conventional process control scheme implemented in several similar
144 plants is present. The operation of the two-stage acid gas abatement system is monitored by
145 the continuous acquisition of flue gas composition data at the measurement points PM1, PM2
146 and EM indicated in Fig. 1. **The concentration of the main gas species at the sampling points,**
147 **including the acid pollutants (HCl, SO₂, HF), is measured by Fourier-Transform infrared (FTIR)**
148 **spectrometry, in compliance with CEN/TS 17337 (CEN, 2019), while the flue gas flowrate is**
149 **determined at stack (point EM) by means of S-type Pitot tube velocity measurements.**

150 In both the acid gas abatement stages, the distributed control system (DCS) of the plant
151 controls the solid reactant feed based on the measured inlet and outlet mass flowrates of
152 acid pollutants. A conditional logic selects the reactant feed rate as the maximum of two
153 values, calculated as follows:

- 154 i. *Feedforward criterion.* The calculated feed rate is equal to the stoichiometric demand
155 related to the abatement of the inlet mass flowrates of acid pollutants at PM1,
156 increased by a 10% excess.
- 157 ii. *Feedback criterion.* The feed rate is calculated according to a Proportional Integral (PI)
158 feedback formula based on the difference between a set-point for the outlet HCl
159 concentration and the value measured at PM2.

160 The settings of the feedback control (proportional gain $K_p = 5$ and integral gain $\tau_I = 8$ s)
161 provide an aggressive reaction, i.e. strong excess feed rates of reactant are delivered
162 whenever the outlet HCl concentration exceeds the setpoint. Conversely, when the outlet HCl
163 concentration is lower than the setpoint, the feed rate of reactant does not drop as
164 significantly, because the feedforward criterion takes over. Thus, the combination of the
165 feedforward and feedback criteria as detailed above realises an asymmetrical control action,
166 in which the setpoint is actually treated as a threshold. The feedforward PI control works
167 merely as an environmental safeguard, intended to act only if the feedforward is not capable
168 to maintain the outlet below the given threshold. A survey carried out by the authors involving
169 several Italian companies (HERAmbiente, HestAmbiente, IREN, Brianza Energia Ambiente)
170 evidenced that this control strategy is typical of WtE acid gas abatement units, as the
171 objective is to avoid any spike in outlet HCl resulting from a variation in the inlet HCl load
172 coming from waste combustion (Muratori et al., 2020).

173

174 **2.3 Drawbacks of the reference control system**

175 The typical behaviour of the control system described in section 2.2 is shown in Fig. 2. Most
176 of the time the control operates in feedforward mode and the feed rate of solid reactant is
177 proportional to the inlet HCl load. However, when the outlet HCl flowrate exceeds its setpoint,
178 the feedback mode takes over, imposing a relevant excess in feed rate to bring the HCl outlet
179 back under the threshold as soon as possible. This behaviour determines a peak in reactant
180 consumption but generates also unintended instability in the outlet HCl flow rate. As
181 pinpointed by the arrows in Fig. 2, the spike of reactant feed manages to quickly reduce the
182 outlet HCl flow rate, but such a reduction is often followed by a swift rebound of outlet HCl
183 to high values that triggers another activation of the feedback control, resulting in another

184 spike of reactant feed. Since the layers of solid reactant accumulated over time on the fabric
185 filter are known to play a major role in the overall acid gas removal action (Kim et al., 2017;
186 Wu et al., 2004), the spikes of reactant feed might be detrimental because they induce
187 unstable operation of the filter (Saleem and Krammer, 2012), activating frequent filter
188 cleaning and reducing the residence time of reactant on the filter. The unstable HCl flow rate
189 at the outlet of the 1st stage can in turn disturb the operation of the 2nd stage of acid gas
190 removal.

191 In general, this control does not include the minimisation of reactant feed as a criterion and
192 does not realise a rational use of reactant.

193

194 3 Methodology

195 3.1 Framework

196 Fig. 3 summarises the methodology developed to analyse the performance of alternative
197 process control strategies for DSI, aimed at environmental and economic optimisation. The
198 core element of the methodology is the development of a process simulation that allows
199 exploring alternative control settings in a virtual console, while reducing the need for full-
200 scale test-runs at the real plant. The process simulation duplicates into a software
201 environment the process units and the control system of the actual facility. As sketched in Fig.
202 3, building the simulation required: i) to reproduce the HCl removal process with a process
203 model; and ii) to simulate the control structure of the DSI unit. The first task required the
204 identification of an appropriate mathematical model for the description of the reaction
205 process (see section 3.2) and its training and validation on plant data collected from test-runs

206 (see section 3.3). The second task was performed replicating the control architecture of the
207 plant, briefly outlined in section 2.2, with a Simulink block diagram (see section 3.4).

208 The reliability of the simulation is validated considering the operating process control set-up
209 in the real plant and comparing the outputs of the simulation with those recorded in the plant
210 during normal operation, using the actual data as the input for the simulation. Once validated,
211 the simulation can be used to screen and tune alternative control strategies, eventually
212 leading to a new tuned control strategy that may be tested in the real plant, as in the test
213 case that will be introduced in section 4.

214 Besides conventional indicators of process control performance, specific environmental and
215 economic indicators (section 3.5) were defined to allow a comprehensive assessment of the
216 performance of the alternative control strategies.

217

218 **3.2 Selection of data-driven process model and input variables**

219 As mentioned above, a mathematical model is required to reproduce the process dynamics
220 in the simulation. The process model needs to predict how the instantaneous HCl removal
221 efficiency varies depending on the inlet HCl concentration and the feed of solid reactant.
222 Given the intrinsic unsteady nature of the process, this task can be addressed only with a
223 dynamic model capable of handling the rapidly changing operating conditions (e.g. variability
224 of HCl concentration due to variability of waste composition). Existing simplified stationary
225 models of acid gas removal that are typically applied for process optimisation studies
226 (Harriott, 1990; Dal Pozzo et al., 2016) are clearly not apt for this task. On the other hand,
227 phenomenological models (Antonioni et al., 2016; Foo et al., 2017; Montagnaro et al., 2016)
228 that describe rigorously the kinetic and mass transfer phenomena involved in the gas-solid
229 reaction process were typically derived from laboratory-scale data and are not suitable to

230 simulate full-scale systems, as stated by Gutiérrez Ortiz and Ollero (2008) and Gassner et al.
231 (2014).

232 Therefore, a data-driven approach was chosen. A system identification procedure was
233 performed to estimate the structure and the parameters of the model from observed input-
234 output plant data (Ljung, 2010). A simple input-output polynomial model, *i.e.* the linear auto-
235 regressive exogenous (ARX) model, was selected as base for the system identification. ARX
236 models have already demonstrated to be reliable tools in emission control problems, e.g. in
237 the prediction of NO_x (Smrekar et al., 2013) or SO_x (Choi et al., 2002) emissions from coal-
238 fired boilers. They are appreciated for their transparency and ease of interpretation (Akinola
239 et al., 2019). The general form of an ARX model is the following:

240

$$241 \quad y(t) = a_1 y(t-1) + \dots + a_{n_a} y(t-n_a) + \sum_i [b_{1,i} u_i(t-n_k) + \dots + b_{n_b,i} u_i(t-n_{k,i}-n_{b,i}+1)] + e(t) \quad (4)$$

242

243 where y is the output variable, u_i are the i input variables considered in the model, and e is
244 the white-noise disturbance value. The values a and b are the model parameters, which can
245 be represented in compact form in the parameter vector θ :

246

$$247 \quad \theta = [a_1 \dots a_{n_a} \ b_{1,i} \dots b_{n_b,i}]' \quad (5)$$

248

249 This model structure implies that the output variable y at time t is predicted as a linear
250 combination of past output values (autoregressive part of the model) and current and past
251 values of the input variables (exogenous part of the model). The parameters n_a and $n_{b,i}$ are,
252 respectively, the number of past output samples and the number of past input samples (for
253 each input variable i) considered for the prediction of the current output. The model can also

254 consider input delay terms $n_{k,i}$, i.e. the number of input samples that occur before the input
255 affects the output (also known as the dead time of the system). The use of past observations
256 in the prediction of the output allows approximating also derivative terms by difference
257 quotients, thus enabling the reproduction of the dynamics of the modelled system. The
258 numbers n_a , $n_{b,i}$ and $n_{k,i}$ are known as hyperparameters and represent the order of the model,
259 i.e. they indicate the number of parameters to optimise in the training of the model.

260 For the sake of simplicity, a two-input single-output ARX model was chosen for the present
261 study. The modelled output y is the HCl molar flowrate in the flue gas leaving the DSI system.
262 The two input variables u_i are the inlet HCl molar flowrate and the molar flowrate of $\text{Ca}(\text{OH})_2$
263 fed to the DSI system.

264 In general, other variables might also affect the HCl removal process. The second most
265 abundant acid compound in WtE flue gases, SO_2 , can consume a fraction of the reactant feed
266 (Zhang et al., 2019). Fluctuations in the flue gas flowrate can influence reactant residence
267 time (Hunt and Sewell, 2015). Variations in the operating temperature of the HCl removal
268 stage, e.g. caused by fouling in the heat recovery section upstream, can alter the gas-solid
269 reaction kinetics (Dal Pozzo et al., 2018c). However, variations of temperature and flue gas
270 flowrate are typically limited (see Fig. 2d and 2e) and, in the WtE plant under study, the inlet
271 SO_2 concentration was a couple of orders of magnitude lower than that of HCl. Therefore,
272 these variables were excluded in the formulation of the model.

273

274 **3.3 Calibration of the model**

275 As a data-driven model, the ARX structure requires a specific calibration on data from the
276 actual DSI system modelled. Informative data can be obtained by open-loop tests, in which

277 the control of the system is deactivated and process performance is assessed by varying
278 manually the feed rate of reactant while recording inlet and outlet HCl concentration.

279 The dataset Z^N , formed by N consecutive observations of the input and output variables,
280 obtained from the tests has to be divided in: i) a training set Z_{trn} , used for the estimation of
281 the optimal model parameters; and, ii) a cross-validation set Z_{crv} , used for the selection of the
282 optimal order of the model.

283 A further validation data set, Z_{val} , obtained collecting operating data from the normal, closed-
284 loop operation of the DSI system can be used for the assessment of the performance of the
285 trained model.

286 Denoting as $\hat{y}(t|\theta)$ the output prediction of the model, least-square method is used to
287 estimate the parameter vector θ^* that produces the best fit of the training data Z_{trn} :

$$288 \theta^* = \arg \min\{V(\theta, Z_{trn})\}, \quad \text{where } V(\theta, Z_{trn}) = \frac{1}{N_{trn}} \sum_{t=0}^{N_{trn}-1} (y(t) - \hat{y}(t|\theta))^2 \quad (6)$$

289 The cross-validation compares the performance of models with different orders, each with its
290 optimal parameter vector θ_i^* , estimated from the training set. The best model is the one for
291 which $V(\theta, Z_{crv})$ is the smallest. This procedure helps selecting a model structure without
292 unnecessary complexity (*i.e.* order), as excessively complex models tend to overfit the training
293 set and perform poorly in the cross-validation set. Lastly, the model with order and
294 parameters optimised for the Z_{trn} and Z_{crv} sets can be tested on the validation set Z_{val} and the
295 procedure can go on iteratively until a given threshold of performance is fulfilled.

296

297 **3.4 Virtual console**

298 The process model described in section 3.2 was integrated into a simulation environment,
299 where also the control loop and the other components of the DSI system were cloned as in

300 the real plant. The virtual console simulating the operation of the real DSI system consists of
301 four blocks, as shown in Figure 4.

302 The block “*Data import*” defines the inlet conditions of the simulation (inlet HCl concentration
303 and flue gas flowrate). These may be either actual plant data, collected at the measurement
304 point PM1 (see Fig. 1), or artificial data, created to test the system performance under specific
305 strain.

306 The input data of the “*Data Import*” block are then transferred to the “*DTS*” and “*DCS*” blocks.
307 The “*DTS*” block contains the process model described in section 3.2. The “*DCS*” block
308 simulates the control system described in section 2.2. Specifically, given as input signals the
309 HCl load at the inlet of the DTS (provided by the “*Data Import*” block) and the HCl load at the
310 outlet of the dry treatment system (modelled by the “*DTS*” block), this block evaluates with a
311 clock time of 1 s the command input for the actuator that regulates the feed rate of Ca(OH)₂.

312 The “*Actuator*” block simulates the operation of the screw feeder installed in the real plant.
313 The virtual actuator receives a percentage command of rotational speed calculated by the
314 “*DCS*” block and transforms it into a molar feed rate of solid reactant to the “*DTS*” block,
315 following a linear relationship between percentage command and feed rate that is
316 characteristic of the real feeder. The response of the actuator was modelled as a first order
317 transfer function:

318

$$319 \quad G(s) = \frac{R}{T_m \cdot s + 1} \quad (7)$$

320

321 where T_m is the actuation time of the screw feeder and R is the command to feed rate ratio.

322 This console allows the comparative testing of the behaviour of the DSI system under the
323 default control (section 2.2) or an alternative control, as discussed in the test case described
324 in section 4.

325

326 **3.5 Performance indicators selected to test alternative control strategies**

327 Both conventional indicators for process control performance and specific indicators
328 capturing the environmental and economic performance of the process were defined to allow
329 a comparison of alternative control strategies. The indicators are reported in Table 1
330 alongside their values obtained for the test case that will be introduced in section 4.

331 With respect to conventional process control indicators, these address the stability of the
332 output variables. The *instability of reactant injection*, expressed as the ratio of the CV of
333 reactant injection to the CV of inlet HCl mass flow, measures the time variability of the feed
334 rate of reactant imposed by the control system. All things equal, a control demanding less
335 variable feed rates is preferred as it induces less mechanical stress on the feeding system. The
336 *instability of HCl outlet*, expressed as the ratio of the CV of outlet HCl mass flow to the CV of
337 inlet HCl mass flow, measures the variability of the HCl mass flow at the outlet of the DSI
338 system.

339 Environmental indicators trace the material streams responsible for the indirect
340 environmental burdens of HCl removal: the *specific consumption of reactant*, expressed as
341 mass of reactant injected per mass of removed HCl, and the *specific generation of residues*,
342 expressed as mass of process residues generated per mass of removed HCl. These indicators
343 were monitored both for the Ca-based 1st stage and the bicarbonate-fed 2nd stage of HCl
344 removal, as the stabilisation of control in the 1st stage (object of the study) can also result in
345 a more stable operation for the 2nd stage. Therefore, an indicator of *overall generation of*

346 *residues*, encompassing both treatment stages, was also considered to have a complete
347 picture of the environmental benefit of control optimisation.

348 Lastly, an indicator addressing *overall operating costs* was also estimated, by translating the
349 streams of reactants and residues in operating costs considering their unit costs (see Table
350 S1).

351

352 **4 Test Case**

353

354 **4.1 Definition of the test case**

355 The test facility described in section 2.1 was used to define a test case for the application of
356 the methodology outlined in section 3. An open-loop test-run was used for the calibration of
357 the ARX model, while the accuracy of the resulting virtual console in reproducing the system
358 behaviour under its default control was assessed using several datasets available for the
359 normal operation of the DSI system. An example of alternative control was proposed, tuned
360 in the virtual console, then tested by full-scale test-runs on the real plant. The set of indicators
361 defined in section 3.4 was adopted to quantify the improvements in the stability of process
362 control and the economic and environmental performance.

363

364 **4.2 Calibration of the model and validation of the simulation for the test case**

365 The behaviour of the DSI system of the test facility was studied via step-response tests (Liu
366 and Gao, 2012). Input excitations were applied to the system by varying stepwise the feed
367 rate of $\text{Ca}(\text{OH})_2$. The effect on system behaviour was recorded by continuous monitoring (**30**
368 **s resolution time**) of the outlet HCl concentration (measurement point PM2 in Fig. 1), while
369 the inlet HCl concentration was also recorded (measurement point PM1 in Fig. 1).

370 On the basis of the discussion provided in section 3.2, the ARX model was calibrated
371 considering the molar flowrate of inlet HCl (calculated from the measured inlet HCl
372 concentration and inlet flue gas flowrate) and the feed rate of Ca(OH)₂ as input variables,
373 while the molar flowrate of outlet HCl (product of the measured outlet HCl concentration
374 and outlet flue gas flowrate) is the modelled output.

375 The virtual console including the calibrated process model was then validated, comparing its
376 simulated outlet of HCl with the measured values in four datasets of operation of the DSI
377 system under the reference control, provided the same input data (see section 5.1). The
378 simulation error was quantitatively assessed by calculating a cumulative normalised root
379 mean squared error (RMSE):

$$380 \text{ Normalised RMSE } (t) = \frac{\sqrt{\frac{1}{n(t)} \sum_{i=1}^{n(t)} (y_i - \hat{y}_i)^2}}{\frac{\sum_{i=1}^{n(t)} y_i}{n(t)}} \quad (8)$$

381 where $n(t)$ is the number of measurements/model evaluations at a given time.

382

383 4.3 Selection and tuning of an alternative control

384 Once the accuracy of the simulation results was demonstrated, the virtual console was used
385 to test alternative approaches to the control of HCl removal operation. In this test case, the
386 control logic described in section 2.2 (named in the following as “conventional control”) was
387 substituted with a simple feedback control (named in the following as “alternative control”).
388 Recalling Fig. 2, the conventional control is built to suppress any overrun of the setpoint of
389 outlet HCl concentration with a spike of Ca(OH)₂ feed. The consequences of such approach,
390 as illustrated in section 2.3, are an excess consumption of Ca(OH)₂ and unstable inlet
391 conditions for the 2nd HCl removal stage fed with NaHCO₃, which, again, lead typically to an

392 excess consumption of NaHCO_3 . Conversely, a properly tuned control in purely feedback
393 action could limit the variability of both reactant feed and outlet HCl concentration.

394 The proposed feedback control is a simple proportional integral (PI) control. As the HCl inlet
395 concentration signal is by nature highly variable and vulnerable to noise contamination
396 (Coleman et al., 2019), the introduction of a derivative (D) control term was avoided, as it
397 could generate system instability (Ting et al., 2008).

398 Hence, in the simulation the two parameters of the feedback control, K_p gain and τ_I integral
399 time, were tuned. The values of the optimised parameters were $K_p = 2$ and $\tau_I = 345$ s.

400

401 **4.4 Performance assessment of the new control at the real plant**

402 Eventually, a comparative assessment of the performance of the conventional and alternative
403 control was carried out at the test facility. The alternative control was easily implemented, by
404 deactivating the feedforward control and updating the feedback settings to the tuned
405 parameters.

406 The test consisted in comparing a period of DSI process operation with the alternative control
407 with a period of operation with the conventional control. The HCl load released by waste
408 combustion can vary widely over time, and any control logic would manage better a low and
409 uniform inlet mass flow of HCl, rather than a high and fluctuating one. Thus, to ensure a
410 proper comparison, a period of operation experiencing an almost equal inlet mass flow of HCl
411 to that present during the test of the alternative control was selected as representative of the
412 conventional control performance.

413 **As a measure of variability of inlet HCl load, the coefficient of variation (CV) of the HCl mass**
414 **flow during the test period was estimated:**

415

416 $CV = \frac{\sigma}{\mu}$ (9)

417

418 where σ and μ are respectively the standard deviation and the mean of the measurements of
419 inlet HCl mass flow during the period of study. It was also ensured that the two periods of DSI
420 operation used for the comparison exhibited a similar CV of HCl mass flow, as it will be
421 discussed in section 5.3. The HCl removal efficiency X was also calculated as follows:

422 $X = \frac{\dot{m}_{HCl,in} - \dot{m}_{HCl,out}}{\dot{m}_{HCl,in}}$ (10)

423 The comparison among the performance of the alternative control strategies was carried out
424 calculating the indicators discussed in section 3.5.

425

426 5 Results and Discussion

427 5.1 Results of the validation of the simulation

428 Figure 5 reports the performance of the virtual console in simulating the behaviour of the
429 conventional process control of the DSI system on a sample dataset (other samples are shown
430 in Figures S1-S3 in the Supporting Information, SI). The percentage command to reactant feed
431 given by the real system and by the simulation are compared in Fig. 5a. Figure 5b compares
432 the measured and the simulated outlet HCl mass flow. The yellow curve represents the set
433 value of outlet HCl mass flow, which is a fluctuating value as it is defined as the product of the
434 fixed setpoint of outlet HCl concentration (see e.g. Fig. 2b) and the variable value of the flue
435 gas flowrate (see e.g. Fig. 2d). Again, it can be noticed that the conventional control treats the
436 set value more like a threshold than a setpoint, as discussed in section 2.3. Figure 5c plots the
437 cumulative average error of the simulation, represented as a normalised RMSE (introduced
438 in section 4.2). The error increases over time, indicating a loss of performance of the process

439 model nested in the simulation, that is typical of error accumulation in models of
440 autoregressive nature (Bazghaleh et al., 2013; Nelles, 2020). As evidenced also by the figures
441 in the SI, the error grows faster when outlet HCl fluctuates widely, while it remains almost
442 unchanged and may even decrease during periods of stable operation. It is clear that a simple
443 ARX model, linear by nature, falls short of achieving an accurate instantaneous prediction of
444 HCl outlet, which is the result of a complex and non-linear process involving gas-solid
445 reactions both in duct and on filter bags. Nonetheless, the simulation captures the average
446 system behaviour with acceptable resolution for the objective of the study.

447

448 **5.2 Results of the virtual testing of the alternative control**

449 The simulation was used for the tuning and for the virtual testing of the alternative PI control.
450 The tuning of the alternative control by the methodology outlined in section 4.3 provided the
451 following value for the control parameters: proportional gain $K_p = 2$ and integral time τ_I of
452 345 s. It should be recalled that the PI settings of the feedback component of the conventional
453 control (see section 2.2) are $K_p = 5$ and $\tau_I = 8$ s. The alternative control is less aggressive,
454 with a reduced proportional action and a significantly higher integral time, which lowers the
455 sensitivity of the control action to temporary deviations of the inlet HCl load. Figure 6a
456 illustrates the different behaviour of the alternative control strategy compared to the
457 conventional process control, on a data sample of 100 min. The simulation of the alternative
458 control was started during a significant deviation of the measured HCl outlet concentration
459 from the set-point value to emphasise the different mode of operation of the two control
460 strategies. The feed rate variations imposed by the alternative control strategy are markedly
461 smoother than those of the conventional control. The proposed strategy accepts momentary
462 upticks in the HCl outlet concentration, whereas the action of the original control results in

463 spikes of reactant feed. Conversely, the alternative control strategy imposes a slightly higher
464 feed rate than the original control during periods in which the latter operates in the
465 feedforward mode. These opposite behaviours are evident from the plot of cumulated
466 reactant consumption reported in Fig. 6c. Given that the variability of the reactant feed rate
467 has been highlighted in section 2.3 as one of the main causes of inefficient reactant
468 exploitation in the DTS, the alternative control strategy appears well suited to rationalise the
469 use of the reactant, thus minimising the resulting generation of process residues.

470

471 **5.3 Results of the field test of the alternative control**

472 The alternative PI control was implemented in the DCS of the test facility. As outlined in
473 section 4.4, a test run of the new control was carried out and the resulting operational data
474 were compared with a previous period under the conventional process control configuration.
475 The equivalence of action between the two controls was guaranteed by selecting the average
476 value of outlet HCl concentration in the previous day under the conventional control as the
477 setpoint for the test of the alternative control (see Fig. 7b).

478 Two 5-hour data samples with similar inlet flue gas conditions were selected for the
479 comparative assessment. The two time series are shown in Fig. 7a, where it is possible to
480 compare qualitatively the behaviour of the two control strategies, i.e. the feed rate of
481 reactant and the outlet HCl flowrate, depending on the inlet HCl flowrate. The relative
482 performance of the two controls was tracked via the indicators introduced in section 3.5.
483 Table 1 provides the list of the indicators used and the specific values obtained, while Figure
484 7c shows a radar plot comparing the normalised values of the performance indicators of the
485 alternative control to the reference one. Internal normalisation was used to obtain the values
486 shown in the figure. Given the low inlet SO₂ concentrations measured at the plant (in the

487 range 10 – 30 mg/Nm³) and the relatively low reactivity compared to HCl, the effect of SO₂ on
488 system performance is negligible and not discussed in the analysis.

489 First of all, the two 5-hour data samples present highly comparable inlet HCl loads, hence the
490 two controls are tested in a situation of similar stress. As reported in Table 1, the average inlet
491 HCl mass flow rate in the two periods is equal and its CV is 68% higher during the test of the
492 alternative control, i.e. the selection of data samples is slightly biased in favour of the
493 conventional control.

494 Figure 7 shows that the real behaviour of the proposed PI-only control is in line with what was
495 expected from the virtual simulation (see Fig. 6). The feed rate varies smoothly, with slow
496 corrections in face of any sharp variation in the outlet HCl flow. Conversely, the conventional
497 control reacts aggressively to deviations in the HCl outlet, with the characteristic spikes of
498 reactant feed rate already described in Fig. 2.

499 When the performance indicators introduced in section 3.5 are considered, the parameter
500 instability of reactant injection captures numerically this difference: while the commanded
501 feed rate of the original control shows a CV that is 4.3 times higher than the CV of the inlet
502 HCl molar flow, the CV of the commanded feed rate of the proposed control is only 1.24 times
503 higher (a 71% reduction, see Table 1).

504 At the same time, the specific consumption of reactant in the Ca(OH)₂-fed treatment stage is
505 11% lower with the proposed control. This confirms that the lower aggressivity of the new
506 control settings is not detrimental to the HCl removal efficiency of the system. On the
507 contrary, in the test period, the proposed control managed to achieve the desired HCl
508 removal performance with a significantly lower variability of reactant feed rate, which has the
509 further advantage of reducing the mechanical stress to the screw feeder and the reactant
510 transport system.

511 Another relevant metric is the instability of the outlet HCl flow, defined in section 3.5 as the
512 ratio between the CVs of outlet and inlet HCl molar flow. The proposed PI-only control
513 achieves a 39% reduction in this indicator. This means that the HCl load exiting the $\text{Ca}(\text{OH})_2$ -
514 fed treatment stage is less variable in time, thus the downstream NaHCO_3 -fed stage operates
515 on a less variable HCl inlet and is put in less stressful working conditions. As a consequence,
516 the optimisation of the control in the $\text{Ca}(\text{OH})_2$ stage generates also a 26% reduction in the
517 specific consumption of reactant in the subsequent NaHCO_3 stage (see again Table 1), whose
518 control was not modified.

519 The overall consequence of the increase in efficiency owing to the new PI-only control is the
520 reduction in the production of the solid process residues of HCl removal via both the gas-solid
521 reactions with $\text{Ca}(\text{OH})_2$ and NaHCO_3 . The new control achieves a 7% and a 22% reduction in
522 the generation of process residues, respectively in the 1st and 2nd treatment stages. The
523 overall effect is a 13% reduction of the amount of process waste generated by the HCl removal
524 operation. A further confirmation of this effect can be observed in figure S4 in the SI, which
525 shows the simulated action of the conventional control system considering the inlet HCl load
526 for the 5-hour dataset collected during the test-run. The figure evidences that the multiple
527 activations of the feedback mode would have caused a higher reactant consumption.

528

529 **5.4 Discussion**

530 In the light of the indicators in Table 1, the alternative control strategy tuned in the virtual
531 simulation was demonstrated to improve the overall economic and environmental
532 performance of the system. The consumption of reactants and the generation of process
533 residues were lowered in both the treatment stages, by increasing the efficiency of reactant
534 delivery. It was thus demonstrated that the main drawback of dry acid gas removal, i.e. the

535 required high excess of reactant, can be partially mitigated by introducing specific process
536 control strategies. In particular, for a multistage system as that of the test facility, it is worth
537 highlighting that an intervention limited to the 1st treatment stage can produce benefits also
538 on the 2nd stage, by enabling a more efficient operation thanks to the lowered variability of
539 the inlet HCl.

540 The alternative control strategy, based on a PI feedback control, however, has clear
541 limitations: even if the simple feedback action reduces the variability of HCl load compared
542 to the conventional control, the instability with respect to a setpoint is still quite high. More
543 advanced control strategies could offer further improvements. Nonetheless, the proposed
544 solution achieved the results in Table 1 with minimal need of full-scale testing and no
545 significant change in the control architecture of the system, demonstrating the ease of
546 implementation of better solid waste and reactant management via control optimisation.

547 The results obtained show that the procedure developed for the test of alternative control
548 strategies, based on a virtual console, and the metric introduced, based on the performance
549 indicators listed in Table 1, provide an effective approach to allow the improvement of the
550 environmental and economic operational performance of acid gas treatment systems.

551

552 6 Conclusions

553 With increasingly strict limits on the emission of airborne pollutants as HCl, the flue gas
554 treatment sections in WtE installations are experiencing problems of excessive consumption
555 of reactants and related high generation of solid residues destined to landfilling, which lead
556 to non-negligible indirect environmental burdens. By considering a reference state-of-the-art
557 acid gas removal system, the present study demonstrated that a standard process control

558 approach based exclusively on the suppression of HCl emissions might be a suboptimal
559 solution in terms of economic and environmental performance. A simple methodology based
560 on virtual simulation and limited full-scale test-runs allowed identifying and tuning an
561 alternative control strategy that achieved a reduction in the generation of solid process
562 residues equal to 7% in the optimised $\text{Ca}(\text{OH})_2$ -fed 1st stage of HCl removal and 13% in the
563 overall two-stage treatment line with respect to the original control configuration, while
564 maintaining the same HCl emission performance at stack.

565 Despite the relevant advantages in terms of reactant economy, a limitation of the proposed
566 solution is that it only partially alleviates the fluctuations in the HCl concentration at the outlet
567 of the 1st treatment stage, which are intrinsic to the WtE context. More advanced process
568 control strategies, taking into account process disturbances other than inlet pollutant
569 concentration and reactant feed rate, could be the key to develop plant-specific highly
570 performant model-based control schemes. However, the present study evidenced that
571 process control optimisation is a promising area of improvement in the management of WtE
572 flue gas treatment, not only to improve stable operation, but also to increase significantly the
573 economic and environmental performance of DSI processes without hindering the
574 compliance to emission limits at stack.

575

576 **References**

- 577 Akinola, T.E., Oko, E., Gu, Y., Wei, H.-L., Wang, M., 2019. Non-linear system identification
578 of solvent-based post-combustion CO₂ capture process. *Fuel* 239, 1213-1223.
- 579 Antonioni, G., Dal Pozzo, A., Guglielmi, D., Tugnoli, A., Cozzani, V., 2016. Enhanced
580 modelling of heterogeneous gas-solid reactions in acid gas removal dry processes. *Chem.*
581 *Eng. Sci.* 148, 140-154.
- 582 Ardolino, F., Boccia, C., Arena, U., 2020. Environmental performances of a modern waste-
583 to-energy unit in the light of the 2019 BREF document. *Waste Manage.* 104, 94-103.
- 584 Arena, U., 2015. From waste-to-energy to waste-to-resources: The new role of thermal
585 treatments of solid waste in the Recycling Society. *Waste Manage.* 37, 1-2.
- 586 Bagheri, M., Esfilar, R., Golchi, M.S., Kennedy, C.A., 2020. Towards a circular economy: A
587 comprehensive study of higher heat values and emission potential of various municipal
588 solid wastes. *Waste Manage.* 101, 210-221.
- 589 Bal, M., Reddy, T.T., Meikap, B.C., 2019. Removal of HCl gas from off gases using self-
590 priming venturi scrubber. *J. Haz. Mat.* 364, 406-418.
- 591 **Bazghaleh, M., Mohammadzaheri, M., Grainger, S., Cazzolato, B., Lu, T.-F., 2013. A new**
592 **hybrid method for sensorless control of piezoelectric actuators. *Sensors and Actuators A:***
593 ***Physical* 194, 25-30.**
- 594 Beylot, A., Hochar, A., Michel, P., Descat, M., Ménard, Y., Villeneuve, J., 2018. Municipal
595 Solid Waste Incineration in France: An Overview of Air Pollution Control Techniques,
596 Emissions, and Energy Efficiency. *J. Ind. Ecol.* 22, 1016-1026.
- 597 Bogush, A., Stegemann, J.A., Wood, I., Roy, A., 2015. Element composition and
598 mineralogical characterisation of air pollution control residue from UK energy-from-waste
599 facilities. *Waste Manage.* 36, 119-129.
- 600 **CEN, 2019. CEN/TS 17337:2019 – Stationary source emissions - Determination of mass**
601 **concentration of multiple gaseous species - Fourier transform infrared spectroscopy.**
602 **European Committee for Standardization, Bruxelles, Belgium.**
- 603 Choi, S., Yoo, C., Lee, I.-B., 2002. SO_x monitoring and neural net classification in the power
604 plant. *J. Environ. Eng.* 128, 911-918.
- 605 Cignitti, S., Mansouri, S.S., Sales-Cruz, M., Jensen, F., Huusom, J.K., 2016. Dynamic
606 Modeling and Analysis of an Industrial Gas Suspension Absorber for Flue Gas
607 Desulfurization. *Emiss. Control Sci. Technol.* 2, 20-32.
- 608 Coleman, M.D., Ellison, M., Robinson, R.A., Gardiner, T.D., Smith, T.O.M., 2019.
609 Uncertainty requirements of the European Union's Industrial Emissions Directive for
610 monitoring sulfur dioxide emissions: Implications from a blind comparison of sulfate
611 measurements by accredited laboratories. *J. Air Waste Manage. Assoc.* 69, 1070-1078.
- 612 Dal Pozzo, A., Moricone, R., Tugnoli, A., Cozzani, V., 2019. Experimental Investigation of
613 the Reactivity of Sodium Bicarbonate toward Hydrogen Chloride and Sulfur Dioxide at Low
614 Temperatures. *Ind. Eng. Chem. Res.* 58, 6316-6324.

615 Dal Pozzo, A., Lazazzara, L., Antonioni, G., Cozzani, V., 2020. Techno-economic
616 performance of HCl and SO₂ removal in waste-to-energy plants by furnace direct sorbent
617 injection. *J. Haz. Mat.* 394, 122518.

618 Dal Pozzo, A., Guglielmi, D., Antonioni, G., Tugnoli, A., 2018a. Environmental and
619 economic performance assessment of alternative acid gas removal technologies for
620 waste-to-energy plants. *Sust. Prod. Consumption* 16, 202-215.

621 Dal Pozzo, A., Armutlulu, A., Rekhtina, M., Müller, C.R., Cozzani, V. 2018b. CO₂ Uptake
622 Potential of Ca-Based Air Pollution Control Residues over Repeated Carbonation-
623 Calcination Cycles. *Energy Fuels* 32, 5386-5395.

624 Dal Pozzo, A., Giannella, M., Antonioni, G., Cozzani, V., 2018c. Optimization of the
625 economic and environmental profile of HCl removal in a municipal solid waste incinerator
626 through historical data analysis. *Chem. Eng. Trans.* 67, 463-468.

627 Dal Pozzo, A., Guglielmi, D., Antonioni, G., Tugnoli, A., 2017. Sustainability analysis of dry
628 treatment technologies for acid gas removal in waste-to-energy plants. *J. Clean. Prod.* 162,
629 1061-1074.

630 Dal Pozzo, A., Antonioni, G., Guglielmi, D., Stramigioli, C., Cozzani, V., 2016. Comparison
631 of alternative flue gas dry treatment technologies in waste-to-energy processes. *Waste*
632 *Manage.* 51, 81-90.

633 Damgaard, A., Riber, C., Fruergaard, T., Hulgaard, T., Christensen, T.H., 2010. Life-cycle-
634 assessment of the historical development of air pollution control and energy recovery in
635 waste incineration. *Waste Manage.* 30, 1244-1250.

636 De Greef, J., Villani, K., Goethals, J., Van Belle, H., Van Caneghem, J., Vandecasteele, C.,
637 2013. Optimising energy recovery and use of chemicals, resources and materials in
638 modern waste-to-energy plants. *Waste Manage.* 33, 2416-2424.

639 Dong, J., Jeswani, H.K., Nzihou, A., Azapagic, A., 2020. The environmental cost of
640 recovering energy from municipal solid waste. *Appl. Energy* 267, 114792.

641 Ephraim, A., Ngo, L.D., Pham Minh, D., Lebonnois, D., Peregrina, C., Sharrock, P., Nzihou,
642 A., 2019. Valorization of Waste-Derived Inorganic Sorbents for the Removal of HCl in
643 Syngas. *Waste Biomass Valorization* 10, 3435-3446.

644 Foo, R., Berger, R., Heiszwolf, J.J., 2016. Reaction Kinetic Modeling of DSI for MATS
645 Compliance. In: Proceedings of the Power Plant Pollutant Control and Carbon
646 Management "MEGA" Symposium, Baltimore, MD, USA, 16–19 August 2016

647 Gassner, M., Nilsson, J., Nilsson, E., Palmé, T., Züfle, H., Bernero, S., 2014. A data-driven
648 approach for analysing the operational behaviour and performance of an industrial flue
649 gas desulphurisation process. *Computer Aided Chem. Eng.* 33, 661-666.

650 Gerassimidou, S., Velis, C.A., Williams, P.T., Castaldi, M.J., Black, L., Komilis, D., 2020.
651 Chlorine in waste-derived solid recovered fuel (SRF), co-combusted in cement kilns: A
652 systematic review of sources, reactions, fate and implications. *Critical Reviews in*
653 *Environmental Science and Technology*, in press.

654 Goodall, P.; Sharpe, R.; West, A., 2019. A data-driven simulation to support
655 remanufacturing operations. *Computers in Industry* 105, 48-60.

656 Guo, Y., Xu, Z., Zheng, C., Shu, J., Dong, H., Zhang, Y., Weng, W., Gao, X., 2019. Modeling
657 and optimization of wet flue gas desulfurization system based on a hybrid modeling
658 method. *J. Air Waste Manage. Assoc.* 69, 565-575.

659 Gutiérrez Ortiz, F.J., Ollero, P., 2008. A realistic approach to modeling an in-duct
660 desulfurization process based on an experimental pilot plant study. *Chem. Eng. J.* 141,
661 141-150.

662 Harriott, P., 1990. A Simple Model for SO₂ Removal in the Duct Injection Process. *J. Air
663 Waste Manage. Assoc.* 40, 998-1003.

664 **Hartman, M., Svoboda, K., Pohorely, M., Syc, M., 2013. Thermal Decomposition of Sodium
665 Hydrogen Carbonate and Textural Features of Its Calcines. *Ind. Eng. Chem. Res.* 52, 10619-
666 10626.**

667 **Hunt, G., Sewell, M., 2015. Utilizing Dry Sorbent Injection Technology to Improve Acid Gas
668 Control. In: 34th International Conference on Thermal Treatment Technologies &
669 Hazardous Waste Combustors, Houston, TX, USA, 20-22 October 2015**

670 Iizuka, A., Morishita, Y., Shibata, E., Takatoh, C., Cho, H., 2020. Basic Study of the Reaction
671 of Calcium Hydroxide with Hydrogen Chloride Using Single Crystals. *Ind. Eng. Chem. Res.*
672 59, 9699-9704.

673 Kameda, T., Tochinai, M., Kumagai, S., Yoshioka, T., 2020. Treatment of HCl gas by cyclic
674 use of Mg–Al layered double hydroxide intercalated with CO₃²⁻. *Atmospheric Pollution
675 Res.* 11, 290-295.

676 Kim, K.-D., Jeon, S.-M., Hasolli, N., Lee, K.-S., Lee, J.-R., Han, J.-W., Kim, H.T., Park, Y.-O.,
677 2017. HCl removal characteristics of calcium hydroxide at the dry-type sorbent reaction
678 accelerator using municipal waste incinerator flue gas at a real site. *Korean J Chem Eng*
679 34, 747-756.

680 Kockmann, N., 2019. Digital methods and tools for chemical equipment and plants. *Reaction
681 Chemistry and Engineering* 4, 1522-1529.

682 Lausset, C., Cherubini, F., del Alamo Serrano, G., Becidan, M., Strømman, A.H., 2016.
683 Life-cycle assessment of a Waste-to-Energy plant in central Norway: Current situation and
684 effects of changes in waste fraction composition. *Waste Manage.* 58, 191-201.

685 Liu, T., Gao, F., 2012. Step Response Identification of Stable Processes. In: Liu, T., Gao, F.,
686 *Industrial Process Identification and Control Design*, Springer-Verlag London, London, UK.

687 Liu, S., Sun, L., Zhu, S., (...), Chen, X., Zhong, W., 2020. Operation strategy optimization of
688 desulfurization system based on data mining. *Appl. Mathematical Modelling* 81, 144-158.

689 Ljung, L., 2010. Perspectives on system identification. *Annual Reviews in Control* 34, 1-12.

690 Margallo, M., Taddei, M.B.M., Hernández-Pellón, A., Aldaco, R., Irabien, A., 2015.
691 Environmental sustainability assessment of the management of municipal solid waste
692 incineration residues: A review of the current situation. *Clean Technol. Environ. Policy* 17,
693 1333-1353.

694 Montagnaro, F., Balsamo, M., Salatino, P., 2016. A single particle model of lime sulphation
695 with a fractal formulation of product layer diffusion. *Chem. Eng. Sci.* 156, 115-120.

696 Muratori, G., Dal Pozzo, A., Antonioni, G., Cozzani, V., 2020. Application of Multivariate
697 Statistical Methods to the Modelling of a Flue Gas Treatment Stage in a Waste-to-energy
698 Plant. *Chem. Eng. Trans.* 82, 397-402.

699 Nelles, O., 2020. *Nonlinear System Identification: From Classical Approaches to Neural*
700 *Networks, Fuzzy Models, and Gaussian Processes.* Springer Nature, Berlin, Germany.

701 Neuwahl, F., Cusano, G., Gomez Benavides, J., Holbrook, S., Roudier, S., 2019. Best
702 Available Techniques (BAT) Reference Document for Waste Incineration. EUR 29971 EN.
703 doi:10.2760/761437

704 Ouda, O.K.M., Raza, S.A., Nizami, A.S., Rehan, M., Al-Waked, R., Korres, N.E., 2016. Waste
705 to energy potential: A case study of Saudi Arabia. *Renewable Sustainable Energy Reviews*
706 61, 328-340.

707 Peng, H., Ozaki, T., Toyoda, Y., Shioya, H., Nakano, K., Haggan-Ozaki, V., Mori, M., 2004.
708 RBF-ARX model-based nonlinear system modeling and predictive control with application
709 to a NO_x decomposition process. *Control Engineering Practice* 12, 191-203.

710 Quina, M.J., Bontempi, E., Bogush, A., Schlumberger, S., Weibel, G., Braga, R., Funari, V.,
711 Hyks, J., Rasmussen, E., Lederer, J., 2018. Technologies for the management of MSW
712 incineration ashes from gas cleaning: New perspectives on recovery of secondary raw
713 materials and circular economy. *Sci. Total Environ.* 635, 526-542.

714 Saleem, M., Krammer, G., 2012. On the Stability of Pulse-Jet Regenerated-Bag Filter
715 Operation. *Chemical Engineering and Technology* 35, 877-884.

716 Smrekar, J., Potočnik, P., Senegačnik, A., 2013. Multi-step-ahead prediction of NO_x
717 emissions for a coal-based boiler. *Appl. Energy* 106, 89-99.

718 Ting, C.-H., Chen, H.-H., Yen, C.-C., 2008. A PID ratio control for removal of HCl/SO_x in flue
719 gas from refuse municipal incinerators. *Control Engineering Practice* 16, 286-293.

720 Van Caneghem, J., Van Acker, K., De Greef, J., Wauters, G., Vandecasteele, C., 2019.
721 Waste-to-energy is compatible and complementary with recycling in the circular
722 economy. *Clean Technol. Environ. Policy*, in press.

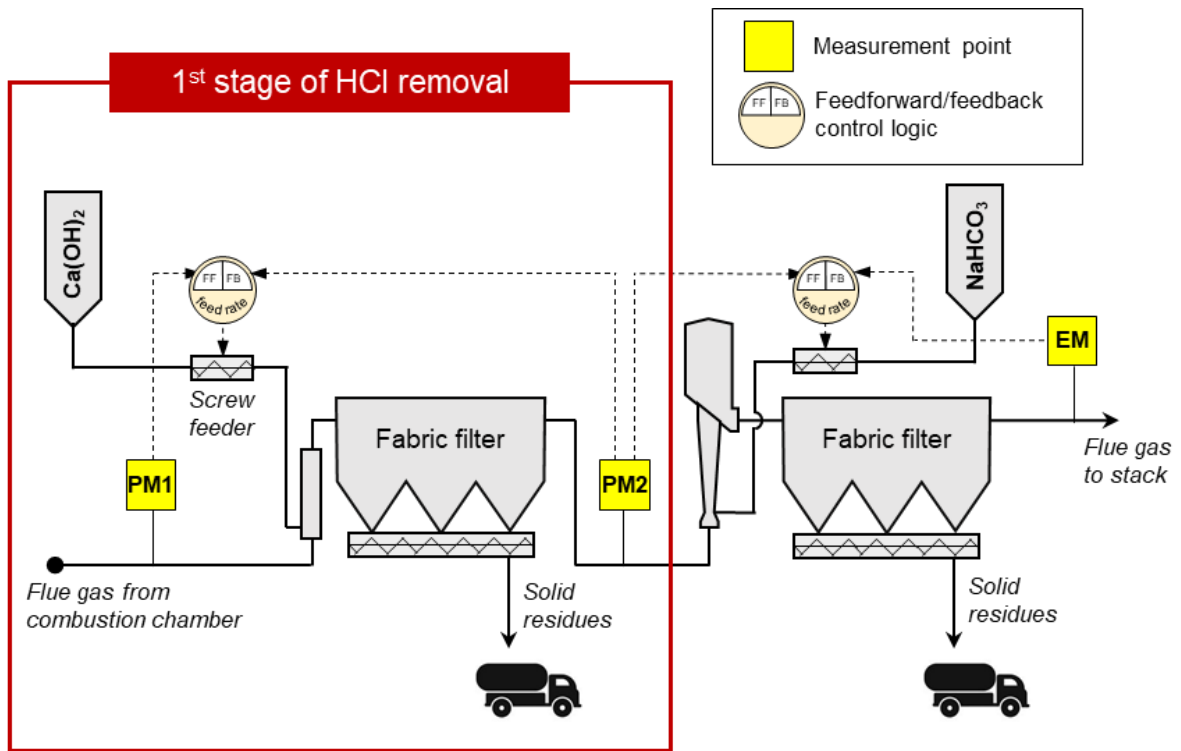
723 Vehlow, J., 2015. Air pollution control systems in WtE units: An overview. *Waste Manage.*
724 37, 58-74.

725 Wu, C., Kang, S.-J., Keener, T.C., Lee, S.-K., 2004. A model for dry sodium bicarbonate duct
726 injection flue gas desulfurization. *Advances in Environmental Research* 8, 655-666.

727 Yang, N., Damgaard, A., Scheutz, C., Shao, L.-M., He, P.-J., 2018. A comparison of chemical
728 MSW compositional data between China and Denmark. *J. Environ. Sci.* 74, 1-10.

729 Zhang, H., Yu, S., Shao, L., He, P., 2019. Estimating source strengths of HCl and SO₂
730 emissions in the flue gas from waste incineration. *J. Environ. Sci.* 75, 370-377.

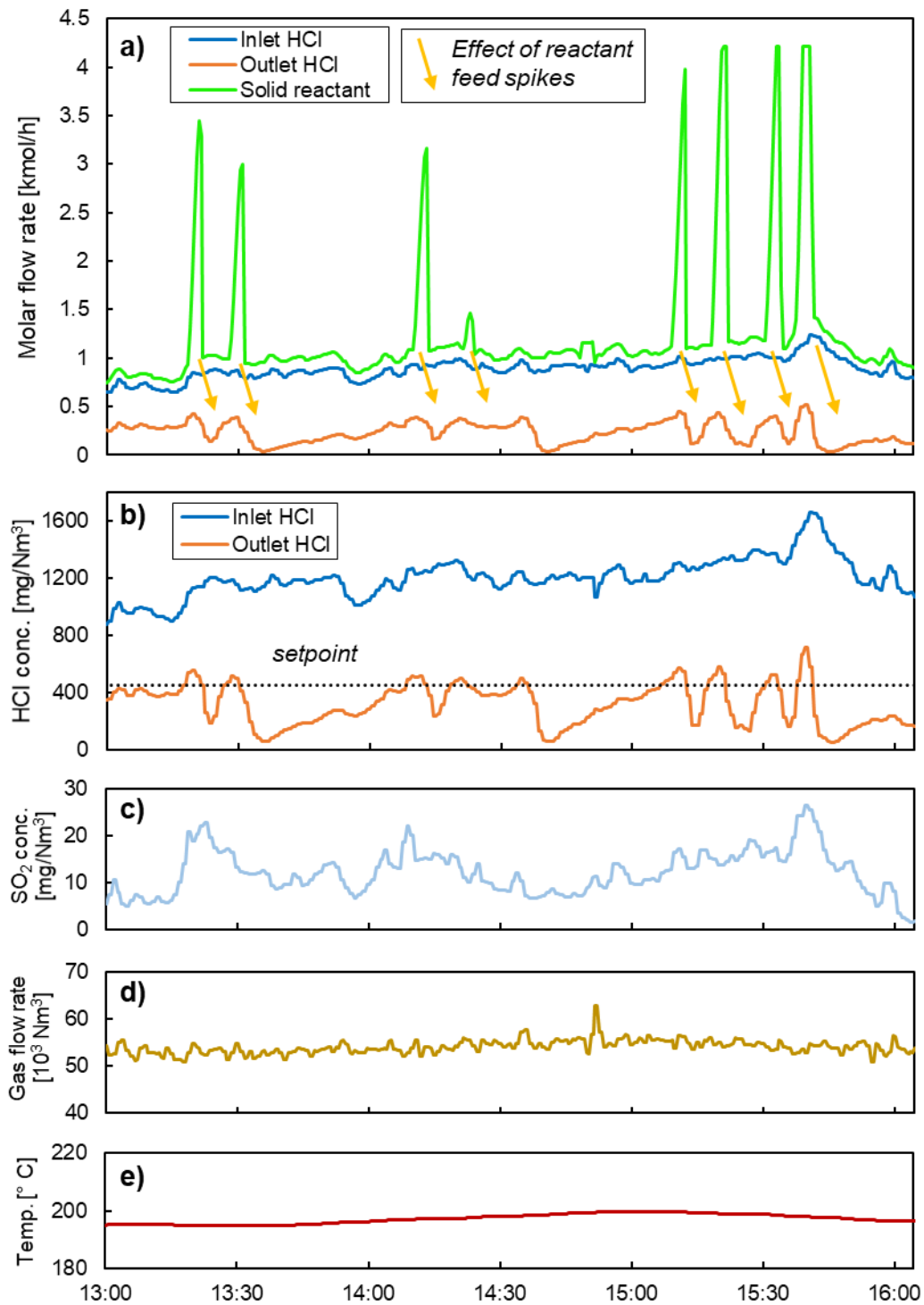
731
732
733
734
735



738

739 **Figure 1.** Scheme of the two-stage acid gas abatement system of the test facility considered,
 740 including measurement points of flue gas composition (PM1, PM2 = process measurement,
 741 EM = measurement at stack) and control loops for reactant feed rate. Control optimization of
 742 1st stage (red box in the figure) was the object of the study.

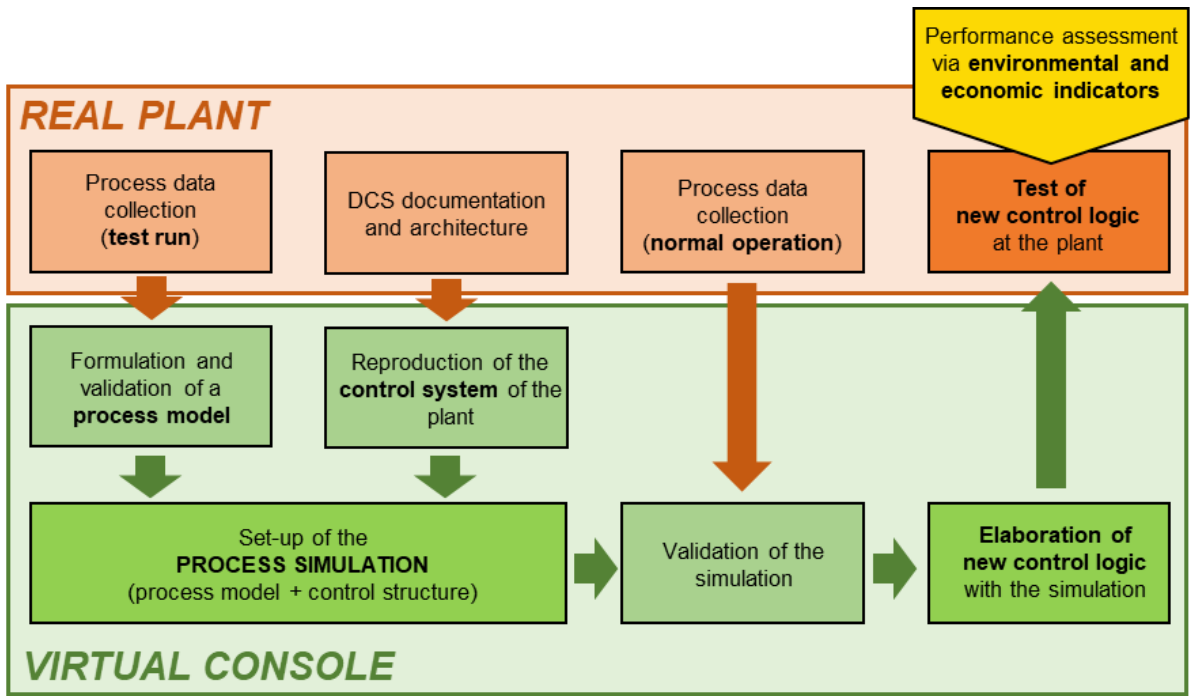
743



744

745 **Figure 2.** Data recorded by the distributed control system (DCS) of an Italian WtE facility
 746 showing: a) the typical trend of inlet and outlet HCl flowrate and solid reactant feed rate
 747 during normal operation of the 1st stage acid gas removal unit applying the conventional
 748 process control strategy; b) threshold setpoint with respect to HCl inlet and outlet
 749 concentrations; c) SO₂ concentration; d) flue gas flowrate; e) operating temperature.

750



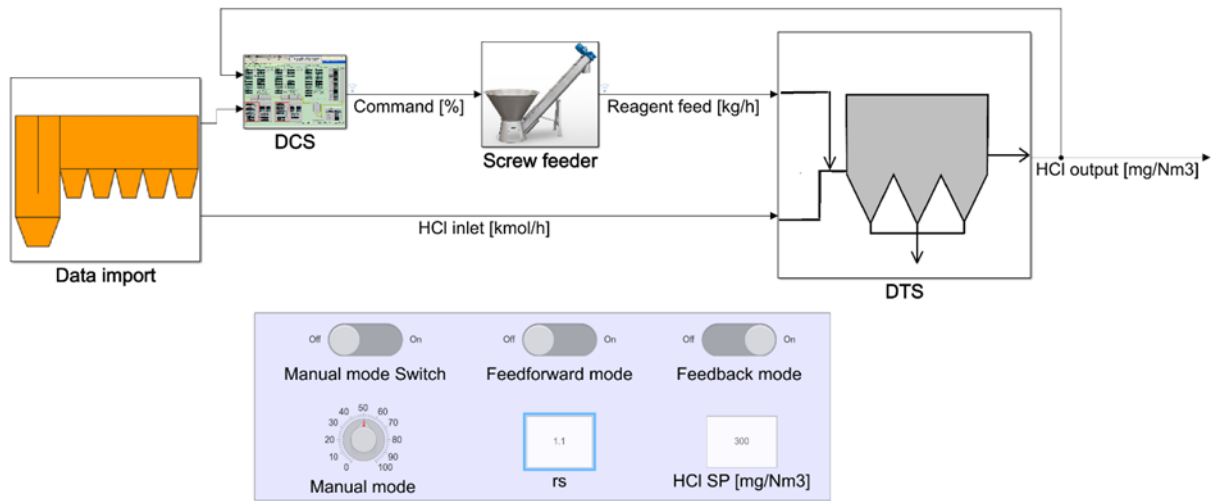
751

752 **Figure 3.** Methodology developed for testing and tuning of improved process control

753 strategies.

754

755

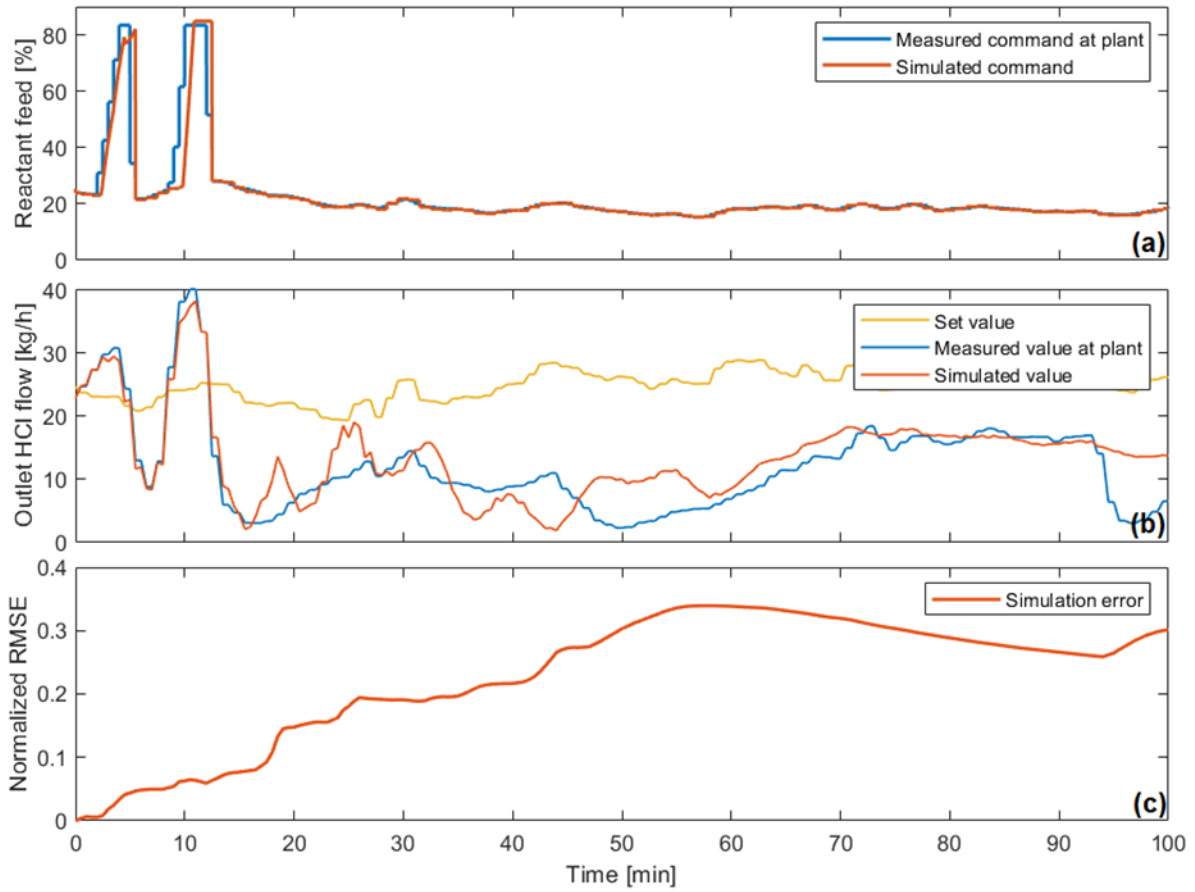


756

757 **Figure 4.** Virtual console developed to simulate the DSI process (1st stage of the acid gas

758 removal system in Fig. 1) using the Simulink[®] software tool.

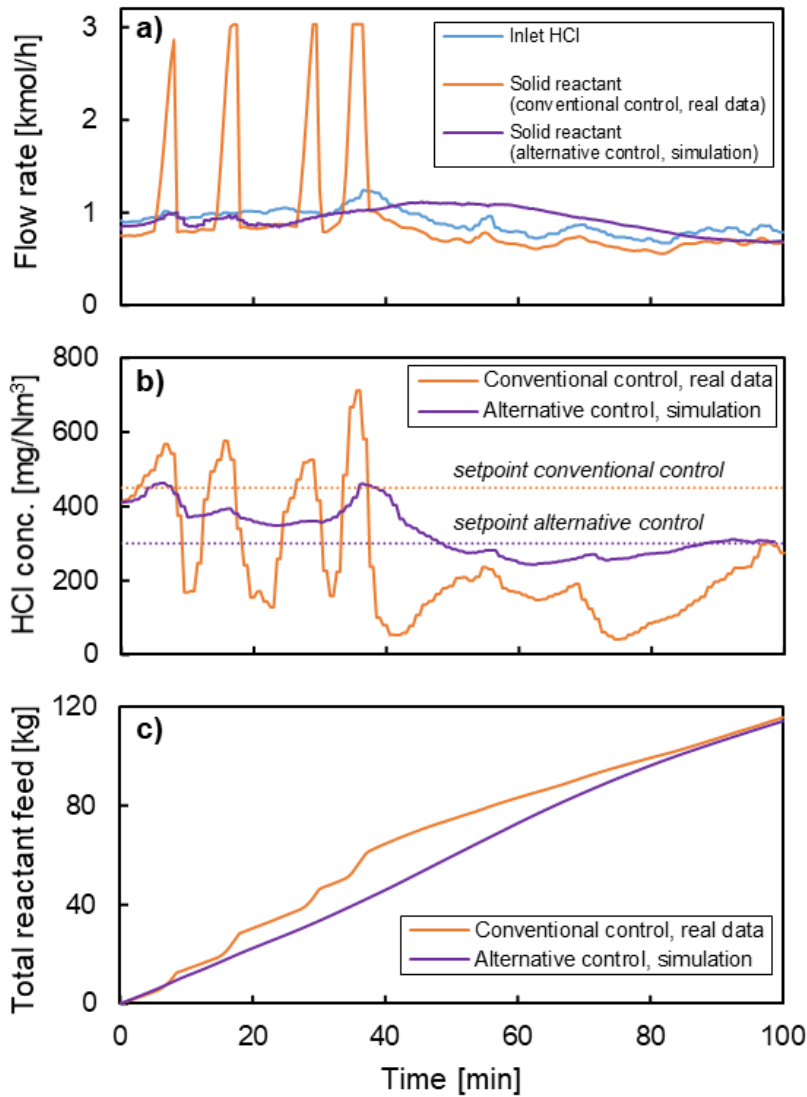
759



760
761

762 **Figure 5.** Performance of the virtual console in simulating the behaviour of the conventional
 763 control of the system: a) measured vs. simulated command of reactant feed, b) measured vs.
 764 simulated outlet HCl flow rate, compared to the set value of the control, c) cumulative average
 765 error of the simulation.

766



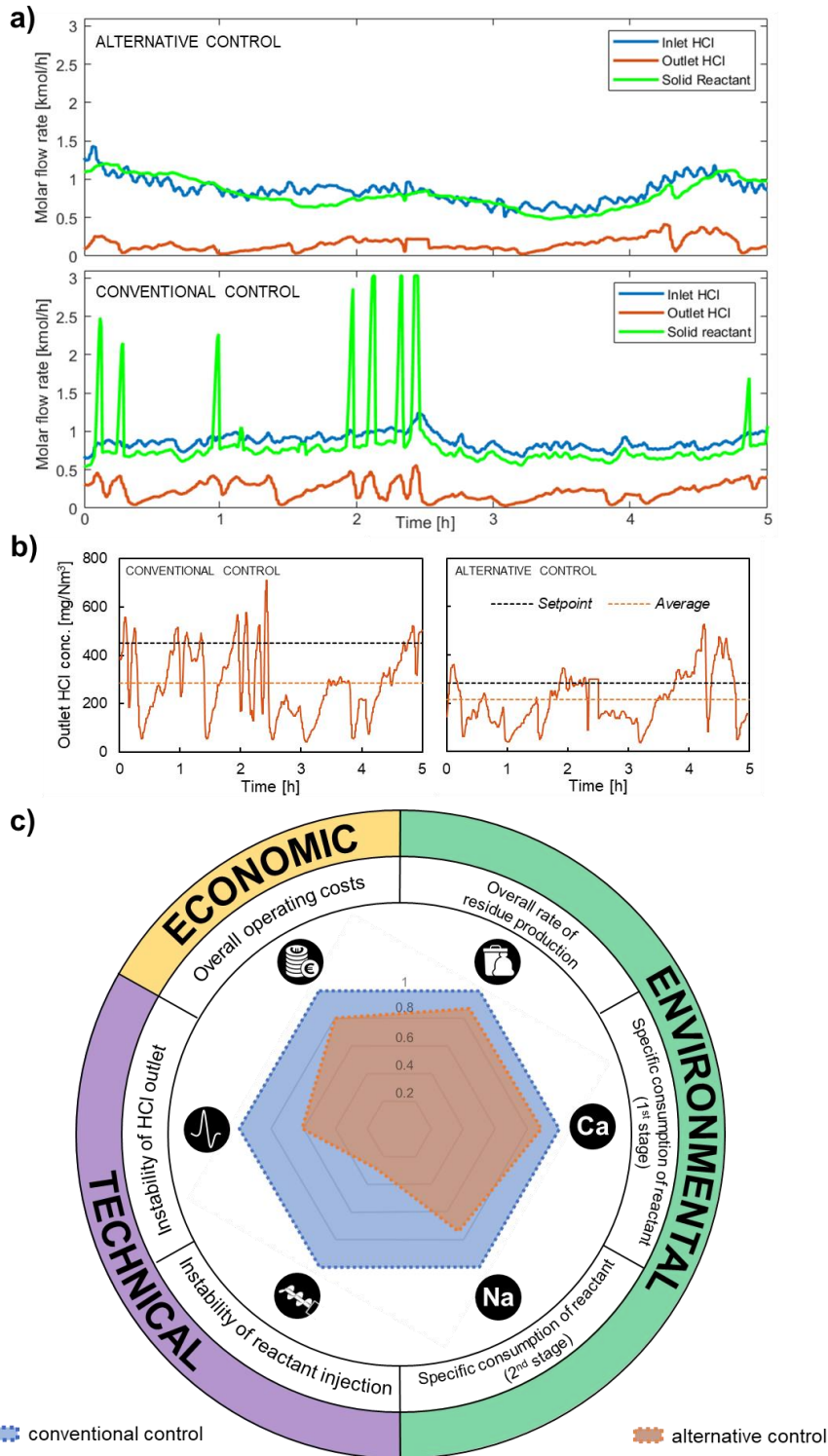
767

768 **Figure 6.** a) Simulation of the reactant feed rate by the alternative PI control strategy

769 compared to the conventional process control on a sample dataset; b) deviation of the outlet

770 HCl concentration from the respective setpoints, c) resulting cumulated reactant consumption.

771



772

773 **Figure 7.** Results of test-run: a) 5-hour data samples obtained during alternative process
 774 control and conventional process control operation under a similar HCl input, b) outlet HCl
 775 concentration in the two 5-hour data samples, c) comparison between the normalised
 776 performance indicators of the alternative process control strategy to the conventional process
 777 control.

778 **Table 1.** Performance of the alternative control strategy vs. the conventional process control
 779 monitored according to the performance indicators introduced in section 3.5.

Parameter or indicator		Test period		Δ
		Conventional control	Alternative control	
Inlet HCl mass flow rate (kg/h)	μ	64.4	64.4	-
	CV	0.12	0.19	+68%
Feed rate of reactant, Ca(OH) ₂ (kg/h)	μ	61.1	60.0	-2%
	CV	0.49	0.24	-52%
Outlet HCl mass flow rate (kg/h)	μ	17.2	12.5	-27%
	CV	0.51	0.52	+2%
HCl removal efficiency (%)	μ	75.8	82.3	+9%
	CV	11.2	8.5	-24%
Instability of reactant injection (CV of Ca(OH) ₂ feed rate / CV of inlet HCl)		4.27	1.24	-71%
Instability of HCl outlet (CV of outlet HCl / CV of inlet HCl)		4.4	2.7	-39%
Specific consumption of reactant (1 st stage) (kg of Ca(OH) ₂ fed / kg of HCl removed)		1.30	1.16	-11%
Specific generation of residues (1 st stage) (kg of residues / kg of HCl removed)		1.80	1.67	-7%
Specific consumption of reactant (2 nd stage) (kg of NaHCO ₃ fed / kg of HCl removed)		3.85	2.86	-26%
Specific generation of residues (2 nd stage) (kg of residues / kg of HCl removed)		2.55	2.00	-22%
Overall rate of residue production (kg of residues / kg of HCl removed)		2.00	1.73	-13%
Overall economic performance (€ of operating costs / kg of HCl removed)		1.86	1.48	-20%

780

781

Declaration of interests

The authors declare that they have no known competing financial interests or personal relationships that could have appeared to influence the work reported in this paper.

The authors declare the following financial interests/personal relationships which may be considered as potential competing interests:



Click here to access/download

Supplementary Material

Suppl Info WM_Control_revFINAL.docx

